Precise Tracking Control for Articulating Crane: Prescribed Performance, Adaptation, and Fuzzy Optimality by Nash Game

Zheshuo Zhang, *Member, IEEE*, Bangji Zhang, Dongpu Cao, *Member, IEEE*, and Hui Yin, *Member, IEEE*

***Abstract*—Articulating crane (AC) is used in various industrial activities. The articulated multisection arm exacerbates nonlinearities and uncertainties, making the precise tracking control challenging. This study proposes an adaptive prescribed performance tracking control (APPTC) for AC to robustly fulfill the task of precise tracking control, with adaptation to resist time-variant uncertainties, whose bounds are unknown but lie in prescribed fuzzy sets. Particularly, a state transformation is applied to simultaneously track the desired trajectory and satisfy the prescribed performance. Adopting the *fuzzy set theory* to describe uncertainties, APPTC does not invoke any IF-THEN fuzzy rules. There is no linearizations, or nonlinear cancelation for APPTC, thus making it approximation free. The performance of the controlled AC is twofold. First, deterministic performance in fulfilling the control task is ensured by the Lyapunov analysis using uniform boundedness and uniform ultimate boundedness. Second, fuzzy-based performance is further improved by an optimal design, which seeks the optima of control parameters by formulating a two-player Nash game. The existence of Nash equilibrium is theoretically proved, and its acquisition process is given. The simulation results are provided for validations. This is the first endeavor that explores the precise tracking control for fuzzy AC.**

***Index Terms*—Adaptive control, articulating crane (AC), fuzzy set, Nash game, prescribed performance control, tracking control, uncertainty.**

I. Introduction

VARIOUS work applications in industrial activities, such as aircraft deicing (Fig. 1), electric line maintenance and tree trimming, and use crane [articulating crane (AC)] [1]. The tools or workers at the AC arm head are delivered to the targets by cooperative luffing of the multisection arms. For an intelligent AC, a smooth trajectory for luffing motions is automatically planned; thus, a trajectory-tracking task is demanded for the control system. The articulated multisection arm exacerbates nonlinearities and uncertainties, which usually leads to large tracking errors [2]. For the sake of the uniformity of spraying deicing fluid or the safety of high-altitude workers, excessive tracking error is unacceptable [3], [4], [5]. Therefore, it is essential to design a precise tracking control for AC.

(a) (b)

Fig. 1. AC.

The task of precise tracking control can be achieved by satisfying prescribed transient and steady-state performance (PTSSP), which falls into the well-known prescribed performance control problem [6]. For linear systems, prescribed performance control problem can be solved by analyzing their dynamic model based on the transfer function and state-space methods [7]. However, for nonlinear systems, prescribed performance control problem is still challenging and usually solved by tedious parameter regulations, which is posteriori. Although some efforts have been made in priori prescribed performance control design [8], [9], [10], there is no relative study of prescribed performance control for the complex nonlinear system with articulated multisection arm, like AC. Consequently, explorations on prescribed performance tracking control of AC are worth pursuing.

Uncertainty is inevitable in the AC [11], [12], [13], which may significantly degrade its control performance. The characteristic of AC uncertainties (e.g., the change of loading mass or the wind disturbance) is generally (possibly fast) time variant and bounded with unknown bounds, making the control design of the AC tough [14], [15], [16]. On the other hand,

Manuscript received 12 July 2022; revised 8 December 2022 and 10 March 2023; accepted 29 March 2023. Date of publication 19 April 2023; date of current version 19 December 2023. This work was supported in part by the National Natural Science Foundation of China under Grant 52102434 and Grant 52105096, and in part by the Open Project of State Key Laboratory of Traction Power under Grant TPL2208. This article was recommended by Associate Editor X.-M. Sun. *(Corresponding author: Hui Yin.)*

Zheshuo Zhang is with the Intelligent Transportation System Research Center, Zhejiang University City College, Hangzhou 310000, China, also with the College of Mechanical and Vehicle Engineering, Hunan University, Changsha 410082, China, and also with the State Key Laboratory of Traction Power, Southwest Jiaotong University, Chengdu 610031, Sichuan, China (e-mail: zhangzs@zucc.edu.cn).

Bangji Zhang is with the Intelligent Transportation System Research Center, Zhejiang University City College, Hangzhou 310000, China, and also with the College of Mechanical and Vehicle Engineering, Hunan University, Changsha 410082, China (e-mail: bangjizhang@hnu.edu.cn).

Dongpu Cao is with the School of Vehicle and Mobility, Tsinghua University, Beijing 100080, China (e-mail: dp_cao2016@163.com).

Hui Yin is with the College of Mechanical and Vehicle Engineering, Hunan University, Changsha 410082, China (e-mail: huiyin@hnu.edu.cn).

Color versions of one or more figures in this article are available at https://doi.org/10.1109/TCYB.2023.3264602.

Digital Object Identifier 10.1109/TCYB.2023.3264602

although many studies have been conducted on uncertainty management in the prescribed performance tracking control, most studies [17], [18] assume that the uncertainty is time-invariant or that its bound is known. Accordingly, developing control schemes that address (possibly fast) time-variant uncertainties with unknown bounds for AC requires more in-depth investigation.

Another limitation of most existing methods that address uncertainties of AC is that they fail to utilize the distribution information of uncertainties to balance the system performance and control effort [19], [20], [21], implying the optimal design of control parameters. This leads to a classical problem, that is, how to mathematically describe uncertainties. Hitherto, the probability theory is the most used method to describe uncertainties [22], [23]; however, it may not be well suited to describing the vast majority of uncertainty as it demands a large amount of experimental data [24]. In contrast, the *fuzzy set theory* interprets the uncertainties by degree of occurrence, which can dramatically reduce the need for data amount through expert opinions [25], [26]. Due to safety and cost concern, it is unrealistic to obtain sufficient data for constructing the probability density function in a probability theory through a large number of experiments on AC; thus, the *fuzzy set theory* is more suitable to describe uncertainties of AC [27], [28]. By this, the optimal design of control parameters with uncertainties using the *fuzzy set theory* is a promising way to balance the system performance and control effort of an AC.

This study proposes an adaptive prescribed performance tracking control (APPTC) for an AC that robustly fulfills the task of precise tracking control by satisfying PTSSP, with adaptation to resist (possibly fast) time-variant uncertainties, whose bounds are unknown but lie in prescribed fuzzy sets. Particularly, the desired trajectory and PTSSP are formulated as equality and inequality servo constraints, respectively. A state transformation then merges the equality and inequality servo constraints, resulting in new equality servo constraints. An adaptive tracking control is then designed to render AC to follow the new ones, which does not invoke any IF-THEN fuzzy rules, distinguishing the current study from the conventional T–S or Mamdani-type fuzzy control [29], [30], [31], [32], [33], [34], [35]. A comprehensive uncertainty bound is estimated online by an adaptive law to measure the most conservative influence of the uncertainties. The performance of APPTC for AC is twofold. First, deterministic performance in fulfilling the control task is ensured by the Lyapunov analysis using uniform boundedness and uniform ultimate boundedness. Second, fuzzy-based performance is improved by an optimal design, which seeks the optima of control parameters by formulating a two-player Nash game. This is different from the conventional optimization combining multiple objectives into single one by weights. The existence of a Nash equilibrium (i.e., the optima of tunable parameters) is proved and the procedure of obtaining the Nash equilibrium is provided. Using the proposed control, PTSSP is deterministically guaranteed, and the system performance and control effort of AC are balanced by fuzzy optimality from the Nash game perspective.

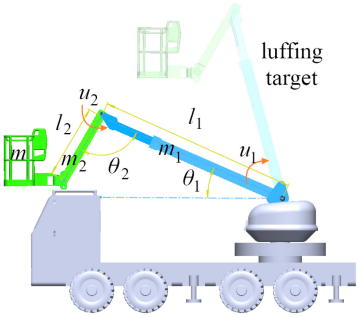

Fig. 2. Dynamic model of AC.

The main contributions are summarized as follows.

1) A comprehensive control design innovatively solves the precise tracking problem for the fuzzy AC system, including the prescribed performance, adaptation, and fuzzy optimality by the Nash game.
2) The Lyapunov analysis ensures the deterministic performance of satisfying PTSSP for the fuzzy AC with uncertainty using uniform boundedness and uniform ultimate boundedness.
3) Adopting fuzzy set to describe uncertainties, a two-player Nash game-oriented optimal design problem is formulated and determined for the optimal gain seeking of APPTC, which is different from conventional optimization of robust control as two cost functions are minimized simultaneously rather than one cost function.

II. Problem Formulation

A. Dynamic Model of AC

Fig. 2 illustrates the model of AC, which consists of two degrees of freedom: θ_1 and θ_2 for luffing angles of the main and auxiliary booms, respectively. The lengths of the main and auxiliary booms are l_1 and l_2, respectively. There is a fixed angle ρ between the auxiliary boom and the platform. m_1, m_2, and m represent the masses of the main boom, auxiliary boom, and platform, respectively.

The dynamic model of AC during luffing with uncertainties can be described as

$$\begin{aligned}\boldsymbol{M}(\boldsymbol{\theta}(t),\boldsymbol{\delta}(t))\ddot{\boldsymbol{\theta}}(t)+\boldsymbol{C}\Big(\dot{\boldsymbol{\theta}}(t),\boldsymbol{\theta}(t),\boldsymbol{\delta}(t)\Big)\dot{\boldsymbol{\theta}}(t)\\+\boldsymbol{G}(\boldsymbol{\theta}(t),\boldsymbol{\delta}(t))=\boldsymbol{u}(t)\end{aligned}\tag{1}$$

where $\boldsymbol{\theta}\in R^2$, $\dot{\boldsymbol{\theta}}\in R^2$, and $\ddot{\boldsymbol{\theta}}\in R^2$ denote the state, velocity, and acceleration vectors, respectively; $t\in R$ denote time, which is an independent variable; and $\boldsymbol{\delta}\in R^n$ denotes the uncertainty vector. In addition, $\boldsymbol{M}\in R^{2\times 2}$, $\boldsymbol{C}\in R^{2\times 2}$, and $\boldsymbol{G}\in R^2$ are related to $\dot{\boldsymbol{\theta}}(t)$, $\boldsymbol{\theta}(t)$, or uncertainties $\boldsymbol{\delta}(t)$, and $\boldsymbol{u}\in R^2$ denotes the control input, which are given as

$$\boldsymbol{M}=\begin{bmatrix}M_{11}&M_{12}\\M_{21}&M_{22}\end{bmatrix},\boldsymbol{C}=\begin{bmatrix}C_{11}&C_{12}\\C_{21}&C_{22}\end{bmatrix}$$
$$\boldsymbol{\theta}=[\theta_1,\theta_2]^T,\boldsymbol{G}=[G_1,G_2]^T,\boldsymbol{u}=[u_1,u_2]^T.$$

Appendix A provides the detailed expressions of the elements for these vectors and matrixes.

Assumption 1: The entries of uncertainties $\boldsymbol{\delta}(t)$ and initial states $\boldsymbol{\theta}_0$ are bounded and lie in the known fuzzy sets as

$$S_{\delta i} = \{(\delta_i, \mu_{\delta i}(\delta_i)) \mid \delta_i \in \Omega_{\delta i}\}, \quad i = 1, 2, \ldots, m$$
$$S_{\theta i} = \{(\theta_{0i}, \mu_{\theta i}(\theta_{0i})) \mid \theta_{0i} \in \Omega_{\theta i}\}, \quad i = 1, 2$$

where $S_{\delta i}$ denotes the fuzzy set for δ_i, $\Omega_{\delta i} \in R$ denotes the universe of discourse of δ_i with fuzzy bound, and $\mu_{\delta i} \to [0, 1]$ is the membership function of $S_{\delta i}$. The membership values "1" and "0" indicate the most "possible" and "impossible" events, respectively. $S_{\theta i}$, θ_{0i}, $\mu_{\theta i}$, and $\Omega_{\theta i}$ have the same meaning. More details of the *fuzzy set theory* can be found in [26].

Remark 1: Assumption 1 applies the *fuzzy set theory* to describe the uncertainties in system (1), which consequently is a fuzzy dynamical system. The term "fuzzy" in the current study is interpreted by the *fuzzy set theory* rather than the *fuzzy logic* theory [30], [33], [35]; thus, the IF-THEN fuzzy rules are not involved. By invoking the IF-THEN fuzzy rules to describe the system model and/or the control, the fuzzy logic theory in control applications is usually to build a surrogate model for the system or the control [14], [30]. In contrast, the fuzzy set theory is to quantify the distribution characteristic of uncertainties, which does not involve approximation. The fuzzy sets for the uncertainties are based on expert opinions and small amount of test data. Due to safety and cost concern, it is unrealistic to obtain sufficient data for constructing the probability density function in a probability theory through a large number of experiments on AC; thus, the *fuzzy set theory* is more suitable to describe the uncertainties of AC [25].

B. Task of Precise Tracking Control

1) Tracking Desired Trajectory: The cycloid curve is an available type of a desired trajectory for states of AC [2]. This curve can generate smooth trajectories $\boldsymbol{P}(t) = [P_1(t), P_2(t)]$

$$P_1(t) = \begin{cases} (\theta_{1d} - \theta_{1s})\left(\frac{t}{t_d} - \frac{\sin(2\pi t/t_d)}{2\pi}\right) + \theta_{1s}, & t < t_d \\ \theta_{1d}, & t \geq t_d \end{cases}$$
$$P_2(t) = \rho - P_1(t) \tag{2}$$

where θ_{1s} and θ_{1d} are the start and goal value of θ_1, respectively, and t_d is the arriving time. Consequently, $\dot{\boldsymbol{P}}(t) = [\dot{P}_1(t), \dot{P}_2(t)]$, $\ddot{\boldsymbol{P}}(t) = [\ddot{P}_1(t), \ddot{P}_2(t)]$

$$\dot{P}_1(t) = \begin{cases} \frac{(\theta_{1d} - \theta_{1s})}{t_d}(1 - \cos(2\pi t/t_d)), & t < t_d \\ 0, & t \geq t_d \end{cases}$$
$$\dot{P}_2(t) = -\dot{P}_1(t).$$
$$\ddot{P}_1(t) = \begin{cases} \frac{2\pi(\theta_{1d} - \theta_{1s})}{t_d^2}\sin(2\pi t/t_d), & t < t_d \\ 0, & t \geq t_d \end{cases}$$
$$\ddot{P}_2(t) = -\ddot{P}_1(t).$$

Remark 2: Since $\lim_{t \to t_d^+} \dot{P}_1(t) = \lim_{t \to t_d^-} \dot{P}_1(t) = 0$ and $\lim_{t \to t_d^+} \ddot{P}_1(t) = \lim_{t \to t_d^-} \ddot{P}_1(t) = 0$, the trajectories in (2) are second-order continuous differentiable in the whole time range, which is critical to the state transformation proposed later.

Let

$$\Xi_i(\boldsymbol{\theta}, t) := \theta_i(t) - P_i(t), \quad i = 1, 2.$$

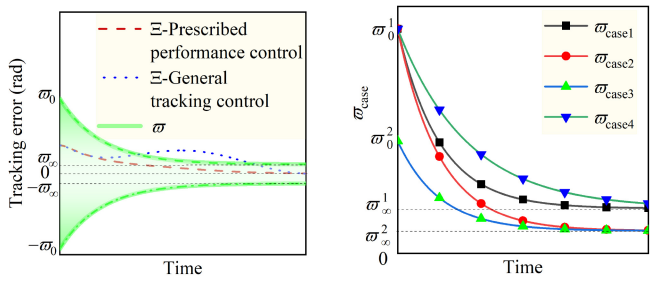

Fig. 3. Effect of the PTSSP parameters on ϖ. (a) Performance satisfying PTSSP. (b) Various PTSSP parameters.

$\Xi_i(\boldsymbol{\theta}, t)$, $(i = 1, 2)$ are the tracking errors and thus can be viewed as the system performance of AC. The system is desired to perform as follows:

$$\Xi_i = 0, \quad i = 1, 2. \tag{3}$$

A control to be designed should drive the system motion to converge to (3).

2) Precise Tracking by Satisfying PTSSP: A task of precise tracking control can be achieved by satisfying PTSSP, that is, that the converging speed is more than a certain value, and the tracking error eventually converges to a predefined area near 0. Nevertheless, it is difficult to guarantee the PTSSP.

The problem of precise tracking control of an AC is formulated by designing a control $\boldsymbol{u} \in R^2$ to drive the states $\boldsymbol{\theta} \in R^2$ of the fuzzy AC tracking the desired trajectories $\boldsymbol{P} \in R^2$ and satisfying the PTSSP indicated by $\varpi_i(t)$, that is, rendering

$$|\Xi_i| < \varpi_i(t) \quad i = 1, 2 \tag{4}$$

where $\varpi_i(t)$ are continuously differentiable, bounded, strictly positive, and decreasing functions as

$$\varpi_i(t) = (\varpi_{i0} - \varpi_{i\infty})e^{-h_i t} + \varpi_{i\infty}. \tag{5}$$

In (5), h_i are positive constants, determining the convergence speed, and ϖ_{i0} are determined, such that the initial values of $\Xi_i(\boldsymbol{\theta}, t)$ satisfy (4). $\lim_{t \to \infty} \varpi_i(t) = \varpi_{i\infty}$; thus, $\varpi_{i\infty}$ determine the ultimate convergence region.

For example, as shown in Fig. 3(a), the upper green line shows the PTSSP function. A prescribed performance control guarantees PTSSP, that is, the red line of "Ξ under prescribed performance control" will not exceed the upper green line of ϖ. However, the general tracking control without considering PTSSP cannot guarantee this, that is, the blue line of "Ξ under general tracking control" may cross over the green line of ϖ. In addition, Fig. 3(b) shows the effect of PTSSP parameters (i.e., ϖ_0, ϖ_∞, and h) on ϖ to further demonstrate how the PTSSP can be specified by adjusting these parameters. Table I lists the parameter values.

Remark 3: Herein, the desired trajectories are formulated as equality servo constraints. Furthermore, the PTSSP is formulated as inequality servo constraints. The next section proposes a priori method to deal with these constraints.

III. Design Procedure

The proposed control design procedure for the AC is summarized in Fig. 4. The desired trajectory and PTSSP are formulated

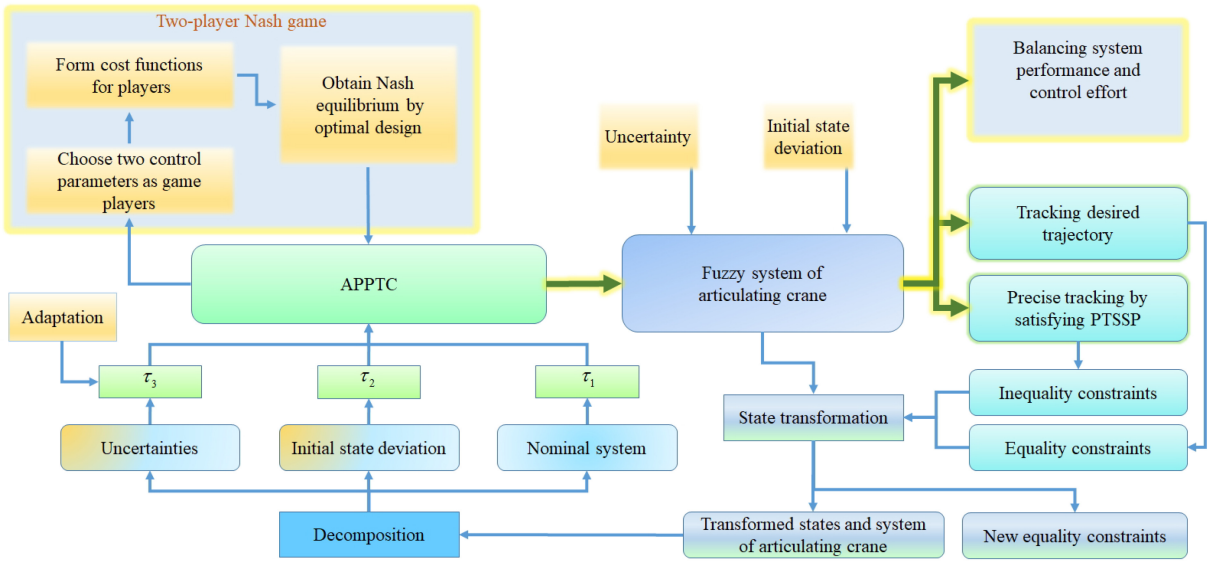

Fig. 4. Control design flowchart.

TABLE I
PTSSP PARAMETER VALUES FOR FOUR DIFFERENT CASES OF ϖ

ϖ of different cases	ϖ_0 value	ϖ_∞ value	h value
ϖ_{case1} for case 1	ϖ_0^1	ϖ_∞^1	h_1
ϖ_{case2} for case 2	ϖ_0^1	ϖ_∞^2	h_1
ϖ_{case3} for case 3	ϖ_0^2	ϖ_∞^2	h_1
ϖ_{case4} for case 4	ϖ_0^1	ϖ_∞^1	h_2

as equality and inequality servo constraints, respectively, and a state transformation is adopted to merge the inequality servo constraints into equality ones, consequently yielding new equality servo constraints. Thus, the control task is transformed into designing a control rendering AC to follow the new equality servo constraints. Based on the uncertainty decomposition, the APPTC is tripartite: τ_1 is the nominal system control; τ_2 is for the initial state deviations; and τ_3 manages uncertainties by an adaptive law. An optimal design of control parameters for fuzzy AC is solved by a two-player Nash game. The cost functions are formulated, the existence of the Nash equilibrium is proved by theoretical analysis, and the procedure of obtaining the Nash equilibrium is given. Substituting the optimal control parameters into the APPTC, PTSSP is deterministically guaranteed and the performance is fuzzily optimized from the Nash game perspective. The proposed approach will drive the fuzzy AC to fulfill the task of precise tracking control, and give the optimal control parameters for the sake of control performance improvement.

IV. APPTC DESIGN FOR AC

This section solves the problem of precise tracking control of AC by proposing an APPTC, which fulfills the control task by satisfying PTSSP.

A. Prescribed Performance

To deal with the inequality servo constraints of PTSSP, a state transformation is proposed to merge the equality (3) and inequality (4) constraints into equality ones. The transformed states are consequently free of inequality constraints. The state transformation is expressed as

$$x_i(\boldsymbol{\theta}, t) := \tan \frac{\pi \Xi_i(\boldsymbol{\theta}, t)}{2\varpi_i(t)} = \tan \frac{\pi(\boldsymbol{\theta}_i(t) - P_i(t))}{2\varpi_i(t)}$$

where $i = 1, 2$. $\boldsymbol{x} = [x_1, x_2]^T$. There is

$$\theta_i = \frac{2\varpi_i}{\pi} \arctan x_i + P_i. \tag{6}$$

Remark 4: When $\Xi_i \to \varpi_i$, $x_i \to \infty$; while $\Xi_i \to -\varpi_i$, $x_i \to -\infty$; if $\Xi_i = 0$, $x_i = 0$, which means that the transformed states x_i are inequality constraint free. Furthermore, this transformation is smooth and bijective (one-to-one). Based on this state transformation, if a control can ensure that $x_i(t)$ is bounded, then the system motion tracks the desired trajectories (3) while satisfying the PTSSP prescription (4).

Substituting (6) into (1) yields the transformed system as

$$\begin{aligned}\boldsymbol{\Theta}(\boldsymbol{x}(t), \boldsymbol{\delta}(t), t)\ddot{\boldsymbol{x}}(t) + \boldsymbol{\Upsilon}\big(\dot{\boldsymbol{x}}(t), \boldsymbol{x}(t), \boldsymbol{\delta}(t), t\big)\dot{\boldsymbol{x}}(t) \\ + \boldsymbol{\Gamma}(\boldsymbol{x}(t), \boldsymbol{\delta}(t), t) = \boldsymbol{u}(t)\end{aligned} \tag{7}$$

where

$$\boldsymbol{\Theta} = \begin{bmatrix} \frac{2\varpi_1}{\pi(1+x_1^2)} M_{11} & \frac{2\varpi_2}{\pi(1+x_2^2)} M_{12} \\ \frac{2\varpi_1}{\pi(1+x_1^2)} M_{21} & \frac{2\varpi_2}{\pi(1+x_2^2)} M_{22} \end{bmatrix}$$

and $\boldsymbol{\Upsilon}\dot{\boldsymbol{x}} + \boldsymbol{\Gamma}$ is shown in Appendix B.

Remark 5: The necessary and sufficient condition for the matrix invertibility is that its determinant is not to be zero. $M_{11}M_{22} - M_{12}M_{21} > 0$ is proved in Appendix A. $|\boldsymbol{M}| = M_{11}M_{22} - M_{12}M_{21} > 0$, hence the invertibility of $\boldsymbol{M}$. $|\boldsymbol{\Theta}| = 4(M_{11}M_{22} - M_{12}M_{21})\varpi_1\varpi_2/(\pi^2(1+x_1^2)(1+x_2^2))$. $\varpi_i > 0$; thus, $|\boldsymbol{\Theta}| > 0$, hence the invertibility of matrix $\boldsymbol{\Theta}$.

The problem formulated in Section II-B2 is equivalent to rendering the transformed AC system (7) to follow the servo constraints:

$$\dot{x}_i(t) + x_i(t) = 0, \quad i = 1, 2 \tag{8}$$

or in matrix form as $\dot{\boldsymbol{x}} = \boldsymbol{c}(\boldsymbol{x})$, with $\boldsymbol{c} = [-x_1, -x_2]^T$. The second-order form can be obtained as $\ddot{\boldsymbol{x}} = \boldsymbol{b}(\dot{\boldsymbol{x}})$, with $\boldsymbol{b} = [-\dot{x}_1, -\dot{x}_2]^T$.

The $\boldsymbol{\Theta}$, $\boldsymbol{\Upsilon}$, and $\boldsymbol{\Gamma}$ in system (7) are decomposed as follows:

$$\begin{cases} \boldsymbol{\Theta}(\boldsymbol{x}, \boldsymbol{\delta}, t) & = \boldsymbol{\Theta}^N(\boldsymbol{x}, t) + \boldsymbol{\Theta}^\Delta(\boldsymbol{x}, \boldsymbol{\delta}, t) \\ \boldsymbol{\Upsilon}(\dot{\boldsymbol{x}}, \boldsymbol{x}, \boldsymbol{\delta}, t) & = \boldsymbol{\Upsilon}^N(\dot{\boldsymbol{x}}, \boldsymbol{x}, t) + \boldsymbol{\Upsilon}^\Delta(\dot{\boldsymbol{x}}, \boldsymbol{x}, \boldsymbol{\delta}, t) \\ \boldsymbol{\Gamma}(\boldsymbol{x}, \boldsymbol{\delta}, t) & = \boldsymbol{\Gamma}^N(\boldsymbol{x}, t) + \boldsymbol{\Gamma}^\Delta(\boldsymbol{x}, \boldsymbol{\delta}, t) \end{cases}$$

where the superscripts N and Δ denote the nominal and uncertain portions, respectively. $\boldsymbol{\Theta}^N > 0$ is always feasible since the nominal portion is the discretion of the designer.

The nominal transformed system can be expressed as

$$\boldsymbol{\Theta}^N(\boldsymbol{x}, t)\ddot{\boldsymbol{x}}(t) + \boldsymbol{\Upsilon}^N(\dot{\boldsymbol{x}}, \boldsymbol{x}, t)\dot{\boldsymbol{x}}(t) + \boldsymbol{\Gamma}^N(\boldsymbol{x}, t) = \boldsymbol{\tau}_1(t)$$

which is servo constraint controllable [11, Th. 1] with respect to constraint (8) for all $(\dot{\boldsymbol{x}}, \boldsymbol{x}, t) \in R^2 \times R^2 \times R$, and the corresponding control can be designed by the U–K approach [21] as

$$\boldsymbol{\tau}_1(\dot{\boldsymbol{x}}, \boldsymbol{x}, t) = \boldsymbol{D}^{-1}(\boldsymbol{x}, t)\big[\boldsymbol{b}(\dot{\boldsymbol{x}}) + \boldsymbol{D}(\boldsymbol{x}, t)\big(\boldsymbol{\Upsilon}^N(\dot{\boldsymbol{x}}, \boldsymbol{x}, t)\dot{\boldsymbol{x}} + \boldsymbol{\Gamma}^N(\boldsymbol{x}, t)\big)\big] \quad (9)$$

where $\boldsymbol{D}(\boldsymbol{x}, t) \coloneqq (\boldsymbol{\Theta}^N(\boldsymbol{x}, t))^{-1}$.

Remark 6: The nonlinear tracking control problem is viewed via the lens of servo constraint. Different from the passive constraint that indicates what the environment should do to the system, the servo constraint indicates what the control should do to the system [19]. Therefore, the constraint force is the control force, and the servo constraint is the control goal.

B. Adaptation

Let the performance index of the transformed system be

$$\boldsymbol{\varepsilon}(\dot{\boldsymbol{x}}, \boldsymbol{x}) \coloneqq \dot{\boldsymbol{x}} - \boldsymbol{c}(\boldsymbol{x})$$

and the following control is proposed to deal with possible initial state deviations:

$$\boldsymbol{\tau}_2(\dot{\boldsymbol{x}}, \boldsymbol{x}, t) = -\frac{\boldsymbol{\Theta}^N(\boldsymbol{x}, t)\boldsymbol{\varepsilon}(\dot{\boldsymbol{x}}, \boldsymbol{x})}{2}. \quad (10)$$

Define

$$\begin{aligned} \boldsymbol{E}(\boldsymbol{x}, \boldsymbol{\delta}, t) &\coloneqq \boldsymbol{\Theta}^N(\boldsymbol{x}, t) \times (\boldsymbol{\Theta}(\boldsymbol{x}, \boldsymbol{\delta}, t))^{-1} - \boldsymbol{I} \\ \Delta\boldsymbol{D}(\boldsymbol{x}, \boldsymbol{\delta}, t) &\coloneqq (\boldsymbol{\Theta}(\boldsymbol{x}, \boldsymbol{\delta}, t))^{-1} - \big(\boldsymbol{\Theta}^N(\boldsymbol{x}, t)\big)^{-1} \\ &= \boldsymbol{D}(\boldsymbol{x}, t)\boldsymbol{E}(\boldsymbol{x}, \boldsymbol{\delta}, t). \end{aligned}$$

Assumption 2: Let

$$W \coloneqq \frac{1}{2}\min_{\boldsymbol{\delta} \in \Omega\delta} \lambda_{\min}\Big(\Delta\boldsymbol{D}\boldsymbol{\Theta}^N + \big(\Delta\boldsymbol{D}\boldsymbol{\Theta}^N\big)^T\Big) \quad (11)$$

there is a fuzzy number $\sigma > -1$ such that for all $(\dot{\boldsymbol{x}}, \boldsymbol{x}, t) \in R^2 \times R^2 \times R$

$$W \geq \sigma \quad (12)$$

where $\lambda_{\min}$ denotes the minimum eigenvalue of the matrix.

As the terms in $\boldsymbol{\Theta}$ and $\boldsymbol{\Upsilon}\dot{\boldsymbol{x}} + \boldsymbol{\Gamma}$ are either constant, states and velocities, or their quadratic, there is a fuzzy vector $\boldsymbol{\alpha} \in (0, \infty)^3$ and a known function

$$\begin{aligned} &Z(\boldsymbol{\alpha}, \dot{\boldsymbol{x}}, \boldsymbol{x}, t) \\ &= \begin{bmatrix} \alpha_1 & \alpha_2 & \alpha_3 \end{bmatrix}\begin{bmatrix} (\|\dot{\boldsymbol{x}}\| + 1)^2 & (\|\boldsymbol{x}\| + 1)^2 & 1 \end{bmatrix}^T \\ &= \boldsymbol{\alpha}^T\tilde{\boldsymbol{Z}}(\dot{\boldsymbol{x}}, \boldsymbol{x}, t) \end{aligned}$$

such that for all $(\dot{\boldsymbol{x}}, \boldsymbol{x}, t) \in R^2 \times R^2 \times R$

$$\begin{aligned} &(1 + \sigma)^{-1} \\ &\max_{\boldsymbol{\delta} \in \Omega\delta} \big\| \Delta\boldsymbol{D}\big(-\boldsymbol{\Upsilon}\dot{\boldsymbol{x}} - \boldsymbol{\Gamma} + \boldsymbol{\tau}_1 + \boldsymbol{\tau}_2\big) + \boldsymbol{D}\big(-\boldsymbol{\Upsilon}^\Delta\dot{\boldsymbol{x}} - \boldsymbol{\Gamma}^\Delta\big)\big\| \\ &\leq Z\big(\boldsymbol{\alpha}, \dot{\boldsymbol{x}}, \boldsymbol{x}, t\big). \end{aligned} \quad (13)$$

Remark 7: The fuzzy numbers σ and $\alpha_i, i = 1, 2, 3$ are relevant to $\boldsymbol{\delta}$. Their membership functions can be determined based on $\mu_i(\boldsymbol{\delta})$, the fuzzy arithmetic, and the decomposition theorem [26].

The **APPTC** is now proposed as

$$\boldsymbol{u} = \boldsymbol{\tau}_1 + \boldsymbol{\tau}_2 + \boldsymbol{\tau}_3. \quad (14)$$

with a component to deal with uncertainties as

$$\begin{aligned} \boldsymbol{\tau}_3(\tilde{\boldsymbol{\alpha}}, \dot{\boldsymbol{x}}, \boldsymbol{x}, t) = &-\gamma(\tilde{\boldsymbol{\alpha}}, \dot{\boldsymbol{x}}, \boldsymbol{x}, t)k_1 Z^2(\tilde{\boldsymbol{\alpha}}, \dot{\boldsymbol{x}}, \boldsymbol{x}, t) \\ &\times \boldsymbol{\Theta}^N(\boldsymbol{x}, t)\boldsymbol{\varepsilon}(\dot{\boldsymbol{x}}, \boldsymbol{x}) \end{aligned} \quad (15)$$

where

$$\gamma(\tilde{\boldsymbol{\alpha}}, \dot{\boldsymbol{x}}, \boldsymbol{x}, t) = \frac{k_2\zeta(\tilde{\boldsymbol{\alpha}}, \dot{\boldsymbol{x}}, \boldsymbol{x}, t)}{k_2\zeta(\tilde{\boldsymbol{\alpha}}, \dot{\boldsymbol{x}}, \boldsymbol{x}, t) + 1} \quad (16)$$

$$\zeta(\tilde{\boldsymbol{\alpha}}, \dot{\boldsymbol{x}}, \boldsymbol{x}, t) = k_1 Z^2(\tilde{\boldsymbol{\alpha}}, \dot{\boldsymbol{x}}, \boldsymbol{x}, t)\big\|\boldsymbol{\varepsilon}(\dot{\boldsymbol{x}}, \boldsymbol{x})\big\|^2 \quad (17)$$

and $k_1, k_2 \in (0, \infty)$ are tunable parameters; $\tilde{\boldsymbol{\alpha}}$ is for estimated value of $\boldsymbol{\alpha}$ and $\tilde{\alpha}_i(t_0) > 0, i = 1, 2, 3$. The adaptive law governing $\tilde{\boldsymbol{\alpha}}$ is given as

$$\dot{\tilde{\boldsymbol{\alpha}}} = k_1\tilde{\boldsymbol{Z}}\|\boldsymbol{\varepsilon}\| - q\tilde{\boldsymbol{\alpha}}. \quad (18)$$

Remark 8: In (14), $\boldsymbol{\tau}_1$ is the nominal system control, $\boldsymbol{\tau}_2$ is for initial state deviations, and $\boldsymbol{\tau}_3$ manages uncertainties with an adaptive law (18). Therefore, the proposed control design is hierarchical. In practical control implementations, the control is computed by $\boldsymbol{\tau}_1 + \boldsymbol{\tau}_2 + \boldsymbol{\tau}_3$ at every instant, encountering both uncertainties and initial condition deviations.

Remark 9: The adaptive law (18) is designed to estimate the unknown uncertainty bounds online, and hence (14) is an adaptive control. The adaptive law is of a leakage type. The first term on the RHS of (18) is for the uncertainty compensation, and the second one is the leak. The initial states $\tilde{\alpha}_i(t_0)$ are strictly positive, and $\tilde{\alpha}_i(t) > 0$ for all $t \geq t_0$ since the first term is always non-negative and the second one renders decaying. Based on the estimated uncertainty bounds, the proposed control is able to compensate uncertainties and guarantee the desired performance under uncertainties, including the gravity-related parameters' uncertainties.

Remark 10: In (18), the leakage rate $q > 0$ is a complement of the compensation rate k_1. The adaptive law can be adjusted by only changing k_1, and $q > 0$ is set as a constant in this study. (k_1, k_2) is then a pair of tunable parameters affecting the control effort.

Theorem 1: Let $\boldsymbol{\psi} \coloneqq [\boldsymbol{\varepsilon}^T, (\tilde{\boldsymbol{\alpha}} - \boldsymbol{\alpha})^T]^T \in R^5$. The control in (14) renders the system (7) the stability performance

of: 1) uniform boundedness and 2) uniform ultimate boundedness

1) For any $r > 0$, there is a $d(r) < \infty$ such that if $\|\boldsymbol{\psi}(t_0)\| \le r$, then $\|\boldsymbol{\psi}(t)\| \le d(r)$ for all $t \ge t_0$.
2) For any $r > 0$ with $\|\boldsymbol{\psi}(t_0)\| \le r$, there is a $\underline{d} > 0$ such that $\|\boldsymbol{\psi}(t)\| \le \bar{d}$ for any $\bar{d} > \underline{d}$ as $t \ge t_0 + T(\bar{d}, r)$, where $0 \le T(\bar{d}, r) < \infty$.

Proof: The Lyapunov function candidate is selected as

$$V(\boldsymbol{\varepsilon}, \tilde{\boldsymbol{\alpha}} - \alpha) = \boldsymbol{\varepsilon}^T\boldsymbol{\varepsilon} + (1+\sigma)(\tilde{\boldsymbol{\alpha}} - \boldsymbol{\alpha})^T k_1^{-1}(\tilde{\boldsymbol{\alpha}} - \boldsymbol{\alpha}). \quad (19)$$

Taking the derivative of V yields

$$\dot{V} = 2\boldsymbol{\varepsilon}^T\dot{\boldsymbol{\varepsilon}} + 2(1+\sigma)(\tilde{\boldsymbol{\alpha}} - \boldsymbol{\alpha})^T k_1^{-1}\dot{\tilde{\boldsymbol{\alpha}}}. \quad (20)$$

For the sake of simplicity, arguments of the functions are largely omitted in the proof, except for some critical ones. For the first term on the RHS of (20)

$$\begin{aligned} 2\boldsymbol{\varepsilon}^T\dot{\boldsymbol{\varepsilon}} &= 2\boldsymbol{\varepsilon}^T(\ddot{\boldsymbol{x}} - \boldsymbol{b}) \\ &= 2\boldsymbol{\varepsilon}^T\left(\boldsymbol{\Theta}^{-1}(\boldsymbol{u} - \boldsymbol{\Upsilon}\dot{\boldsymbol{x}} - \boldsymbol{\Gamma}) - \boldsymbol{b}\right) \\ &= 2\boldsymbol{\varepsilon}^T\left(\boldsymbol{\Theta}^{-1}(\boldsymbol{\tau}_1 + \boldsymbol{\tau}_2 + \boldsymbol{\tau}_3 - \boldsymbol{\Upsilon}\dot{\boldsymbol{x}} - \boldsymbol{\Gamma}) - \boldsymbol{b}\right). \end{aligned}$$

Decompose $\boldsymbol{\Theta}^{-1} = \boldsymbol{D} + \Delta\boldsymbol{D}$ and $-\boldsymbol{\Upsilon}\dot{\boldsymbol{x}} - \boldsymbol{\Gamma} = (-\boldsymbol{\Upsilon}^N\dot{\boldsymbol{x}} - \boldsymbol{\Gamma}^N) + (-\boldsymbol{\Upsilon}^\Delta\dot{\boldsymbol{x}} - \boldsymbol{\Gamma}^\Delta)$, and there is

$$\begin{aligned} &\boldsymbol{\Theta}^{-1}(\boldsymbol{\tau}_1 + \boldsymbol{\tau}_2 + \boldsymbol{\tau}_3 - \boldsymbol{\Upsilon}\dot{\boldsymbol{x}} - \boldsymbol{\Gamma}) - \boldsymbol{b} \\ &= (\boldsymbol{D} + \Delta\boldsymbol{D})(-\boldsymbol{\Upsilon}\dot{\boldsymbol{x}} - \boldsymbol{\Gamma}) + (\boldsymbol{D} + \Delta\boldsymbol{D})(\boldsymbol{\tau}_1 + \boldsymbol{\tau}_2 + \boldsymbol{\tau}_3) - \boldsymbol{b} \\ &= \boldsymbol{D}(-\boldsymbol{\Upsilon}^N\dot{\boldsymbol{x}} - \boldsymbol{\Gamma}^N) + \boldsymbol{D}(\boldsymbol{\tau}_1 + \boldsymbol{\tau}_2) + \boldsymbol{D}(-\boldsymbol{\Upsilon}^N\dot{\boldsymbol{x}} - \boldsymbol{\Gamma}^N) \\ &\quad + \Delta\boldsymbol{D}(-\boldsymbol{\Upsilon}\dot{\boldsymbol{x}} - \boldsymbol{\Gamma} + \boldsymbol{\tau}_1 + \boldsymbol{\tau}_2) + (\boldsymbol{D} + \Delta\boldsymbol{D})\boldsymbol{\tau}_3 - \boldsymbol{b}. \end{aligned}$$

By (9), following is obtained:

$$\boldsymbol{D}(-\boldsymbol{\Upsilon}^N\dot{\boldsymbol{x}} - \boldsymbol{\Gamma}^N) + \boldsymbol{D}\boldsymbol{\tau}_1 - \boldsymbol{b} = 0.$$

Next, by (13)

$$\begin{aligned} &2\boldsymbol{\varepsilon}^T\left(\Delta\boldsymbol{D}(-\boldsymbol{\Upsilon}\dot{\boldsymbol{x}} - \boldsymbol{\Gamma} + \boldsymbol{\tau}_1 + \boldsymbol{\tau}_2) + \boldsymbol{D}(-\boldsymbol{\Upsilon}^\Delta\dot{\boldsymbol{x}} - \boldsymbol{\Gamma}^\Delta)\right) \\ &\le 2\|\boldsymbol{\varepsilon}\|\left\|\Delta\boldsymbol{D}(-\boldsymbol{\Upsilon}\dot{\boldsymbol{x}} - \boldsymbol{\Gamma} + \boldsymbol{\tau}_1 + \boldsymbol{\tau}_2) + \boldsymbol{D}(-\boldsymbol{\Upsilon}^\Delta\dot{\boldsymbol{x}} - \boldsymbol{\Gamma}^\Delta)\right\| \\ &\le 2\|\boldsymbol{\varepsilon}\|(1+\sigma)Z(\boldsymbol{\alpha}, \dot{\boldsymbol{x}}, \boldsymbol{x}, t). \end{aligned} \quad (21)$$

By (10), and performing matrix cancelation, the following is obtained:

$$2\boldsymbol{\varepsilon}^T\boldsymbol{D}\boldsymbol{\tau}_2 = \boldsymbol{\varepsilon}^T\boldsymbol{D}(-\boldsymbol{\Theta}^N\boldsymbol{\varepsilon}) = -\|\boldsymbol{\varepsilon}\|^2. \quad (22)$$

By (15) and (16), the following is obtained:

$$\begin{aligned} &2\boldsymbol{\varepsilon}^T(\boldsymbol{D} + \Delta\boldsymbol{D})\boldsymbol{\tau}_3 \\ &= 2\boldsymbol{\varepsilon}^T\boldsymbol{D}\boldsymbol{\tau}_3 + 2\boldsymbol{\varepsilon}^T\boldsymbol{D}\boldsymbol{E}\boldsymbol{\tau}_3 \\ &= -2\gamma\zeta - 2k_1\gamma\boldsymbol{\varepsilon}^T\Delta\boldsymbol{D}\boldsymbol{\Theta}^N\boldsymbol{\varepsilon}Z^2(\tilde{\boldsymbol{\alpha}}, \dot{\boldsymbol{x}}, \boldsymbol{x}, t). \end{aligned} \quad (23)$$

By (11) and (12), the following is obtained:

$$\begin{aligned} &-2k_1\gamma\boldsymbol{\varepsilon}^T\Delta\boldsymbol{D}\boldsymbol{\Theta}^N\boldsymbol{\varepsilon}Z^2(\tilde{\boldsymbol{\alpha}}, \dot{\boldsymbol{x}}, \boldsymbol{x}, t) \\ &\le -2k_1\gamma\boldsymbol{\varepsilon}^T W\boldsymbol{\varepsilon}Z^2(\tilde{\boldsymbol{\alpha}}, \dot{\boldsymbol{x}}, \boldsymbol{x}, t) \\ &= -2\sigma\gamma\zeta. \end{aligned} \quad (24)$$

Substitute (23) and (24), the following is obtained:

$$2\boldsymbol{\varepsilon}^T(\boldsymbol{D} + \Delta\boldsymbol{D})\boldsymbol{\tau}_3 \le -2(1+\sigma)\gamma\zeta. \quad (25)$$

In total, by (16), (17), (21) (22), and (25), the following is obtained:

$$\begin{aligned} 2\boldsymbol{\varepsilon}^T\dot{\boldsymbol{\varepsilon}} &\le -\|\boldsymbol{\varepsilon}\|^2 + 2(1+\sigma)\|\boldsymbol{\varepsilon}\|Z(\boldsymbol{\alpha}, \dot{\boldsymbol{x}}, \boldsymbol{x}, t) \\ &\quad - 2(1+\sigma)\gamma\zeta \\ &\le -\|\boldsymbol{\varepsilon}\|^2 + 2(1+\sigma)\|\boldsymbol{\varepsilon}\|Z(\boldsymbol{\alpha}, \dot{\boldsymbol{x}}, \boldsymbol{x}, t) \\ &\quad - 2\frac{1}{k_2}\frac{(k_2\zeta)^2 - 1}{k_2\zeta + 1}(1+\sigma) \\ &= -\|\boldsymbol{\varepsilon}\|^2 + 2(1+\sigma)\|\boldsymbol{\varepsilon}\|Z(\boldsymbol{\alpha}, \dot{\boldsymbol{x}}, \boldsymbol{x}, t) \\ &\quad - 2(1+\sigma)\|\boldsymbol{\varepsilon}\|Z(\tilde{\boldsymbol{\alpha}}, \dot{\boldsymbol{x}}, \boldsymbol{x}, t) \\ &\quad + 2(1+\sigma)\|\boldsymbol{\varepsilon}\|Z(\tilde{\boldsymbol{\alpha}}, \dot{\boldsymbol{x}}, \boldsymbol{x}, t) \\ &\quad - 2(1+\sigma)k_1\|\boldsymbol{\varepsilon}(\dot{\boldsymbol{x}}, \boldsymbol{x})Z(\tilde{\boldsymbol{\alpha}}, \dot{\boldsymbol{x}}, \boldsymbol{x}, t)\|^2 \\ &\quad + \frac{2(1+\sigma)}{k_2} \\ &\le -\|\boldsymbol{\varepsilon}\|^2 + 2(1+\sigma)\|\boldsymbol{\varepsilon}\|(\boldsymbol{\alpha} - \tilde{\boldsymbol{\alpha}})^T\tilde{Z} \\ &\quad + \frac{1+\sigma}{2k_1} + \frac{2(1+\sigma)}{k_2}. \end{aligned} \quad (26)$$

Using the adaptive law (18), the following is obtained:

$$\begin{aligned} &2(1+\sigma)k_1^{-1}(\tilde{\boldsymbol{\alpha}} - \boldsymbol{\alpha})^T\dot{\tilde{\boldsymbol{\alpha}}} \\ &\le 2(1+\sigma)(\tilde{\boldsymbol{\alpha}} - \boldsymbol{\alpha})^T\tilde{Z}\|\boldsymbol{\varepsilon}\| \\ &\quad - \frac{2(1+\sigma)\|\tilde{\boldsymbol{\alpha}} - \boldsymbol{\alpha}\|^2 q}{k_1} + \frac{2(1+\sigma)\|\tilde{\boldsymbol{\alpha}} - \boldsymbol{\alpha}\|\|\boldsymbol{\alpha}\|q}{k_1} \\ &= 2(1+\sigma)(\tilde{\boldsymbol{\alpha}} - \boldsymbol{\alpha})^T\tilde{Z}\|\boldsymbol{\varepsilon}\| \\ &\quad - \frac{(1+\sigma)\|\tilde{\boldsymbol{\alpha}} - \boldsymbol{\alpha}\|^2 q}{k_1} \\ &\quad + \frac{(1+\sigma)\left(-\|\tilde{\boldsymbol{\alpha}} - \boldsymbol{\alpha}\|^2 + 2\|\tilde{\boldsymbol{\alpha}} - \boldsymbol{\alpha}\|\|\boldsymbol{\alpha}\|\right)q}{k_1} \\ &\le 2(1+\sigma)(\tilde{\boldsymbol{\alpha}} - \boldsymbol{\alpha})^T\tilde{Z}\|\boldsymbol{\varepsilon}\| \\ &\quad - \frac{(1+\sigma)\|\tilde{\boldsymbol{\alpha}} - \boldsymbol{\alpha}\|^2 q}{k_1} + \frac{(1+\sigma)\|\boldsymbol{\alpha}\|^2 q}{k_1}. \end{aligned} \quad (27)$$

Note that $\|\boldsymbol{\psi}\|^2 = \|\boldsymbol{\varepsilon}\|^2 + \|\tilde{\boldsymbol{\alpha}} - \boldsymbol{\alpha}\|^2$. By (26) and (27), the following is obtained:

$$\begin{aligned} \dot{V} &\le -\|\boldsymbol{\varepsilon}\|^2 - \frac{(1+\sigma)\|\tilde{\boldsymbol{\alpha}} - \boldsymbol{\alpha}\|^2 q}{k_1} \\ &\quad + \frac{(1+\sigma)\|\boldsymbol{\alpha}\|^2 q}{k_1} + \frac{1+\sigma}{2k_1} + \frac{2(1+\sigma)}{k_2} \\ &\le -K_1\|\boldsymbol{\psi}\|^2 + K_2 \end{aligned} \quad (28)$$

where

$$\begin{aligned} K_1 &= \min\left\{1, \frac{(1+\sigma)q}{k_1}\right\} \\ K_2 &= \frac{1+\sigma}{2k_1} + \frac{2(1+\sigma)}{k_2} + \frac{(1+\sigma)\|\boldsymbol{\alpha}\|^2 q}{k_1}. \end{aligned}$$

By invoking the standard arguments on uniform boundedness and uniform ultimate boundedness in [25] and [26], it can be concluded that $\|\boldsymbol{\psi}\|$ is uniformly bounded by

$$d(r) = \begin{cases} R\sqrt{\frac{\iota_2}{\iota_1}} & \text{if } r \le R \\ r\sqrt{\frac{\iota_2}{\iota_1}} & \text{if } r > R \end{cases}$$

$$R = \sqrt{\frac{K_2}{K_1}}$$

where $\iota_1 = \min\{1, k_1^{-1}(1+\sigma)\}$, $\iota_2 = \max\{1, k_1^{-1}(1+\sigma)\}$. Furthermore, uniform ultimate boundedness for $\|\boldsymbol{\psi}\|$ is

$$\underline{d} = R\sqrt{\frac{\iota_2}{\iota_1}}$$

and

$$T(\bar{d}, r) = \begin{cases} 0, & \text{if } r \le \bar{d} \\ \frac{\iota_2 r^2 - (\iota_1^2/\iota_2)\bar{d}^2}{K_1\bar{d}^2(\iota_1/\iota_2) - K_2}, & \text{otherwise.} \end{cases}$$ ■

Remark 11: Theorem 1 ensures that the proposed control guarantees $\boldsymbol{\varepsilon}$ to be bounded. This indicates that the proposed control will render the system motion to converge to (8) and satisfy (4). The control design has no linearizations, nonlinear cancelation, or any other approximations; thus, it is approximation free.

Remark 12: The adaptive control in Section IV-B is also applicable to control the motion of system (1) to converge to the servo constraint (3) accounting for uncertainties. Nevertheless, without the state transformation in the prescribed performance tracking control design, the PTSSP cannot be guaranteed as (4). This will be shown in the later performance validation.

Remark 13: The pair of tunable parameters in control (k_1, k_2) determine the size of UB and UUB, thus the system performance. Recalling Remark 10, (k_1, k_2) also affect the control effort. (k_1, k_2) can determine the overall balance between the system performance and control effort.

V. Fuzzy Optimality by Nash Game

The choice of parameters (k_1, k_2) leads to an optimal design problem of control parameters for fuzzy AC. This section formulates the problem as a Nash game, which requires players to act independently to pursue their own minimum cost, thus leading to the Nash equilibrium.

A. Formulation of Optimal Design Problem of Control Parameters by the Nash Game

Let $J_i(k_1, k_2)$ and $\tilde{D}_i$ be the cost functions and decision sets for players k_1 and k_2, respectively. Each cost function consists of an average fuzzy system performance index and the associated player's control effort. This problem is a two-player game, in which two players can change only their own decision. The first player wants to minimize $J_1(k_1, k_2)$ by choosing k_1 in $\tilde{D}_1$, while the second player wants to minimize $J_2(k_1, k_2)$ by selecting k_2 in $\tilde{D}_2$.

The problem of optimal design of control parameters is formulated as follows: in a game

$$J_{1,2}(k_1, k_2) : \prod_{1,2}^{2} \tilde{D}_{1,2} \to R$$

find the ideal decision $(k_1^*, k_2^*) \in \prod_{1,2}^{2} \tilde{D}_{1,2}$ that satisfies

$$J_{1,2}(k_1^*, k_2^*) \le J_{1,2}(k_1, k_2) \quad \forall (k_1, k_2) \in \prod_{1,2}^{2} \tilde{D}_{1,2}$$

indicating that (k_1^*, k_2^*) simultaneously minimizes all cost functions. Nevertheless, such a utopia may not exist, resulting in a dilemma for the players: How can one find an optimal decision if each player acts independently?

According to Nash, if the players do not cooperate with each other when pursuing their own minimum cost, this game is a noncooperative game, that is, a Nash game. As the opponents' decisions affect a player's cost in a Nash game, players face a problem: When making the "best" decision, what to assume is the opponent's decision? Naturally, a player will assume that the opponent is "rational," that is, without the tendency to "hurt" the other player. This leads to the Nash equilibrium (k_1^*, k_2^*), which is the solution of the problem

$$\begin{aligned} \min_{k_1 \in \tilde{D}_1} &: J_1(k_1, k_2^*) \\ \min_{k_2 \in \tilde{D}_2} &: J_2(k_1^*, k_2). \end{aligned} \tag{29}$$

Remark 14: It should be noted that seeking the Nash equilibrium results in minimizing the cost functions J_1 and J_2 simultaneously. A Nash-game-oriented optimization is clearly different from the conventional optimization issues for the different numbers of cost functions. In addition, this article optimizes the control parameters, which are different from the conventional optimal control [15]. The main disadvantage of a conventional optimal control is that it is difficult to obtain the solution for systems with complex nonlinearities and uncertainties. In contrast, the proposed control parameter optimization is practically feasible for the systems with complex nonlinearities and uncertainties, and the analytical solution can be obtained as shown later.

B. Relationship Between Control Parameters and System Performance

Recalling (19) and (28), one has

$$\begin{aligned} V &= \|\boldsymbol{\varepsilon}\|^2 + k_1^{-1}(1+\sigma)\|\tilde{\boldsymbol{\alpha}} - \boldsymbol{\alpha}\|^2 \\ \dot{V} &\le -\left(\|\boldsymbol{\varepsilon}\|^2 + q(k_1)^{-1}(1+\sigma)\|\tilde{\boldsymbol{\alpha}} - \boldsymbol{\alpha}\|^2\right) + K_2 \\ &\le -\left(\|\boldsymbol{\varepsilon}\|^2 + k_1^{-1}(1+\sigma)\|\tilde{\boldsymbol{\alpha}} - \boldsymbol{\alpha}\|^2\right) + K_2 \\ &= -V + K_2 \end{aligned}$$

where K_2 is expressed in (29), and $0 < q < 1$. For any control start time t_s, any V at time t, $(t \ge t_s)$ has

$$V \le (V_s - K_2)e^{-(t-t_0)} + K_2$$

where $V_s = \|\boldsymbol{\varepsilon}(t_s)\|^2 + k_1^{-1}(1+\sigma)\|\tilde{\boldsymbol{\alpha}}(t_s) - \boldsymbol{\alpha}\|^2$ is the V at t_s. Let

$$\begin{aligned} \eta(\tilde{\boldsymbol{\alpha}}, k_1, k_2, t, t_s) &= \left(V_s(\tilde{\boldsymbol{\alpha}}, k_1, t_s) - K_2(\tilde{\boldsymbol{\alpha}}, k_1, k_2)\right)^{-(t-t_s)} \\ \eta_\infty(\tilde{\boldsymbol{\alpha}}, k_1, k_2) &= K_2(\tilde{\boldsymbol{\alpha}}, k_1, k_2). \end{aligned}$$

Therefore, k_1 and k_2 can be seen as two players in a Nash game, and $\eta(\tilde{\boldsymbol{\alpha}}, k_1, k_2, t, t_s)$ and $\eta_\infty(\tilde{\boldsymbol{\alpha}}, k_1, k_2)$ represent the relationship between k_1, k_2 and the system performance.

C. Cost Functions of the Players

There are three necessary elements in a Nash game: 1) the players are k_1 and k_2; 2) the decision sets $\tilde{D}_1$ and $\tilde{D}_2$ for two players are both $(0, \infty)$; and 3) the cost functions for them are given as follows.

It is proposed that the cost functions for k_1 and k_2 are

$$J_1 := D\left[\int_{t_s}^{\infty} \eta^2 dt\right] + D\left[\eta_\infty^2\right] + k_1^2$$
$$J_2 := D\left[\int_{t_s}^{\infty} \eta^2 dt\right] + D\left[\eta_\infty^2\right] + k_2^2. \tag{30}$$

Remark 15: The players intend to minimize the average fuzzy system performance and control effort simultaneously, implying a balance between the system performance and control effort. In (30), $D[\int_{t_s}^{\infty} \eta^2 dt]$ denotes the value of the overall transient performance (via the integration) from time t_s, and $D[\eta_\infty^2]$ denotes the value of the steady-state performance. In addition, k_1^2 and k_2^2 relate to the control effort.

It can be noticed that the cost functions are also related to the uncertainties described by the *fuzzy set theory*. Based on the D-operation (reviewed in Appendix C)

$$\begin{aligned} &D\left[\int_{t_s}^{\infty} \eta^2 dt\right] \\ &= D\left[(V_s - K_2)^2 \int_{t_s}^{\infty} e^{-(t-t_s)} dt\right] \\ &= \epsilon_1 + \epsilon_2 k_2^{-2} + \epsilon_3 k_2^{-1} + \epsilon_4 k_1^{-1} k_2^{-1} + \epsilon_5 k_1^{-1} + \epsilon_6 k_1^{-2} \\ &D\left[\eta_\infty^2\right] \\ &= D\left[(1+\sigma)\left(\frac{1+2q\|\boldsymbol{\alpha}\|^2}{2k_1} + \frac{2}{k_2}\right)\right]^2 \\ &= \epsilon_7 k_2^{-2} + \epsilon_8 k_1^{-1} k_2^{-1} + \epsilon_9 k_1^{-2} \end{aligned}$$

where $\epsilon_i, (i = 1, 2, \ldots, 9)$ are related to $D[\sigma]$, $D[\|\boldsymbol{\alpha}\|]$, $D[\|\tilde{\boldsymbol{\alpha}}(t_s) - \boldsymbol{\alpha}\|]$, and $D[\|\boldsymbol{\varepsilon}(t_s)\|]$ and given in Appendix D.

Let

$$J_*(k_1, k_2, t_s) := D\left[\int_{t_s}^{\infty} \eta^2 dt\right] + D\left[\eta_\infty^2\right]$$

and rewrite (30) as

$$J_1 = J_* + k_1^2, J_2 = J_* + k_2^2.$$

Remark 16: The fuzzy optimality in the current study is different from the conventional optimization of robust control in two ways. First, (29) incorporates a Nash game to minimize two cost functions (J_1 and J_2) simultaneously, rather than one cost function. Second, (30) is different for the description method of uncertainties, that is, a *fuzzy set theory* is applied.

D. Solution to the Nash Equilibrium

To obtain the solution of (29), take the first-order derivative of $J_1(k_1, k_2^*)$ with respect to k_1, and take the first-order derivative of $J_2(k_1^*, k_2)$ with respect to k_2. Any pair that satisfies (31) and (32) will be in the Nash equilibrium

$$\frac{\partial J_1(k_1, k_2^*)}{\partial k_1} = 0, \frac{\partial J_2(k_1^*, k_2)}{\partial k_2} = 0 \tag{31}$$
$$\frac{\partial^2 J_1(k_1, k_2^*)}{\partial k_1^2} > 0, \frac{\partial^2 J_2(k_1^*, k_2)}{\partial k_2^2} > 0. \tag{32}$$

Remark 17: The existence of a Nash equilibrium should be proved first to avoid the situation of no solution. Nevertheless, [36], [37] did not prove it. To improve this, this study rigorously proves the existence of a Nash equilibrium by theoretical analysis.

Theorem 2: Let

$$J = J_* + k_1^2 + k_2^2$$

and the solution of

$$\min_{k_1 \in \tilde{D}_1, k_2 \in \tilde{D}_2} : J(k_1, k_2) \tag{33}$$

always exists and is also the solution of (29), that is, the Nash equilibrium.

Proof: First, the existence of the solution of (33) should be proved. There is

$$\begin{aligned} J &= J_* + k_1^2 + k_2^2 \\ &= \left[D[\|\boldsymbol{\varepsilon}(t_s)\|]^2 + (1 + D[\sigma])\right. \\ &\qquad \left.\left(\frac{2D\left[\left\|\tilde{\boldsymbol{\alpha}}(t_s) - \boldsymbol{\alpha}\right\|\right]^2 - 2qD[\|\boldsymbol{\alpha}\|]^2 - 1}{2k_1} - \frac{2}{k_2}\right)\right]^2 \\ &\quad + \left[(1 + D[\sigma])\left(\frac{1 + 2qD[\|\boldsymbol{\alpha}\|]^2}{2k_1} + \frac{2}{k_2}\right)\right]^2 + k_1^2 + k_2^2. \end{aligned} \tag{34}$$

Note that the constrained domains $\tilde{D}_1$ and $\tilde{D}_2$ have four boundaries, namely, $k_1 \to 0$, $k_1 \to \infty$, $k_2 \to 0$, and $k_2 \to \infty$. It can be found from (34) that $J = \infty$ at all boundaries. It is known that $\epsilon_i, (i = 1, 2, \ldots, 9)$ are finite values independent to k_1 and k_2. Therefore, J is first-order continuous differentiable (the derivative exists at each point in domains $\tilde{D}_1$ *and* $\tilde{D}_2$). By the extreme value theorem, there always exists a minimum value for J in domains $\tilde{D}_1$ and $\tilde{D}_2$, proving the existence of the solution of (33). ■

Second, it should be proved that the solution of (33) is also the solution of (29). Since $J = J_1 + k_2^2 = J_2 + k_1^2$, there is

$$\frac{\partial J(k_1, k_2)}{\partial k_1} = \frac{\partial J_1(k_1, k_2)}{\partial k_1}, \frac{\partial J(k_1, k_2)}{\partial k_2} = \frac{\partial J_2(k_1, k_2)}{\partial k_2}.$$

The solution of (33) can be obtained by

$$\frac{\partial J_1(k_1, k_2)}{\partial k_1} = 0, \frac{\partial J_2(k_1, k_2)}{\partial k_2} = 0. \tag{35}$$

It can be found that (35) is actually the same equation system as (31). If the solution of (35) exists and they are denoted as $(k_{1i}, k_{2i})(i \in \Omega_i)$, we search among these solution and find the ones $(k_{1j}, k_{2j})(j \in \Omega_j \subseteq \Omega_i)$ that satisfy

$$\left[\begin{array}{cc} \frac{\partial^2 J}{\partial k_1^2} & \frac{\partial^2 J}{\partial k_1 \partial k_2} \\ \frac{\partial^2 J}{\partial k_2 \partial k_1} & \frac{\partial^2 J}{\partial k_2^2} \end{array}\right]\Bigg|_{(k_1, k_2) = (k_{1j}, k_{2j})} > 0$$

thus the local minimum point of $J(k_1, k_2)$. Consequently, the minimum value of J is

$$\min_{k_1 \in \tilde{D}_1, k_2 \in \tilde{D}_2} J(k_1, k_2) = \min_{j \in \Omega_j} J(k_{1j}, k_{2j}).$$

TABLE II
PARAMETERS FOR THE NOMINAL AC

Parameters	Description	Nominal Values	Units
m	Mass of empty platform	350	kg
m_1	Mass of main boom, magnetic induction	1000	kg
m_2	Mass of auxiliary boom	400	kg
l_1	Length of main boom	15	m
l_2	Length of auxiliary boom	4	m
ρ	Fixed angle between the auxiliary boom and the platform	120	degree

Denote the solution of (33) as $(\hat{k}_1, \hat{k}_2)$; one can then obtain

$$J\left(\hat{k}_1, \hat{k}_2\right) = J_1\left(\hat{k}_1, \hat{k}_2\right) + \hat{k}_2^2 = J_2\left(\hat{k}_1, \hat{k}_2\right) + \hat{k}_1^2 \tag{36}$$

and

$$\begin{aligned} &J\left(\hat{k}_1, \hat{k}_2\right) \le J\left(k_1, \hat{k}_2\right) = J_1\left(k_1, \hat{k}_2\right) + \hat{k}_2^2 \\ &J\left(\hat{k}_1, \hat{k}_2\right) \le J\left(\hat{k}_1, k_2\right) = J_2\left(\hat{k}_1, k_2\right) + \hat{k}_1^2 \\ &\forall k_1 \in \tilde{D}_1, k_2 \in \tilde{D}_2. \end{aligned} \tag{37}$$

Substituting (36) into (37) yields

$$\begin{aligned} &J_1\left(\hat{k}_1, \hat{k}_2\right) \le J_1\left(k_1, \hat{k}_2\right),\ J_2\left(\hat{k}_1, \hat{k}_2\right) \le J_2\left(\hat{k}_1, k_2\right) \\ &\forall k_1 \in \tilde{D}_1, k_2 \in \tilde{D}_2. \end{aligned} \tag{38}$$

By (38), $(\hat{k}_1, \hat{k}_2)$ is also the solution of the problem (29), that is, the solution of (33) is also the solution of (29).

In a conclusion, since the solution of (33) always exists, the Nash equilibrium of (29) always exists. If the pair (k_1^*, k_2^*) satisfies the solution of problem (33), it is the Nash equilibrium of the optimal design problem (29).

VI. PERFORMANCE VALIDATION

In this section, the performance of AC using the proposed APPTC method is studied, and the Nash game optimization is also demonstrated. A control task is to move the platform from $\theta_{1s} = 1.2217$ to $\theta_{1d} = 0.1745$ in $t_d = 30$ s while keeping the platform upright, that is, $\theta_{2s} = 0.8727$ and $\theta_{2d} = 1.9199$. The desired trajectories can be obtained by (2). The PTSSP specification can be determined by (5) with $\varpi_{10} = 0.1745$, $\varpi_{1\infty} = 0.0349$, $\varpi_{20} = 0.1396$, and $\varpi_{2\infty} = 0.0175$. With the deviations, the initial states are set as $\theta_{01} = 1.3614$, $\theta_{02} = 0.9599$, $\dot{\theta}_{01} = 0.0017$ rad/s, and $\dot{\theta}_{02} = 0.0017$ rad/s.

The nominal portions of parameters are listed in Table II. The uncertain portions of parameters is described by the *fuzzy set theory*: the uncertain portion of platform mass m^Δ due to different load are close to 50 kg; the uncertain portions of boom mass and length and fixed angle m_1^Δ, m_2^Δ, l_1^Δ, l_2^Δ, and ρ^Δ possibly caused by manufacturing errors are "close to 0". Their associated membership functions are given as (all triangular)

$$\mu_{m^\Delta}(v) = \begin{cases} \frac{v}{50}, & 0 \le v \le 50 \\ 2 - \frac{v}{50}, & 50 \le v \le 100 \end{cases}$$

$$\mu_{m_1^\Delta}(v) = \begin{cases} \frac{v}{20} + 1, & -20 \le v \le 0 \\ -\frac{v}{20} + 1, & 0 \le v \le 20 \end{cases}$$

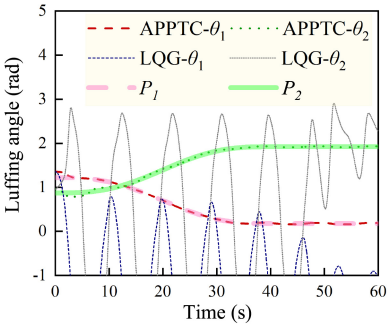

Fig. 5. Luffing angles by APPTC of AC system with initial state deviations and uncertainties.

$$\mu_{m_2^\Delta}(v) = \begin{cases} \frac{v}{8} + 1, & -8 \le v \le 0 \\ -\frac{v}{8} + 1, & 0 \le v \le 8 \end{cases}$$

$$\mu_{l_1^\Delta}(v) = \begin{cases} \frac{10v}{3} + 1, & -\frac{3}{10} \le v \le 0 \\ -\frac{10v}{3} + 1, & 0 \le v \le \frac{3}{10} \end{cases}$$

$$\mu_{l_2^\Delta}(v) = \begin{cases} \frac{100v}{8} + 1, & -\frac{8}{100} \le v \le 0 \\ -\frac{100v}{8} + 1, & 0 \le v \le \frac{8}{100} \end{cases}$$

$$\mu_{\rho^\Delta}(v) = \begin{cases} \frac{v}{2} + 1, & -2 \le v \le 0 \\ -\frac{v}{2} + 1, & 0 \le v \le 2. \end{cases}$$

In the simulations, the uncertainty bounds are within the prescribed fuzzy sets, echoing Assumption 1. The uncertainties applied for the AC in the simulations are $m^\Delta = 50 + 50\sin t$, $m_1^\Delta = 20\sin(0.2\pi t)$, and $m_2^\Delta = 8\sin(20\pi t)$ for masses, $l_1^\Delta = 0.3\sin(0.2\pi t)$ and $l_2^\Delta = 0.08\sin(0.2\pi t)$ for boom lengths, and $\rho^\Delta = 2\sin(0.2\pi t)$ for the fixed angel. The changing frequency of m_2^Δ is deliberately chosen as 10 Hz to stand for the fast time-variant uncertainties. The uncertainty bound is unknown and estimated by the adaptive law.

A. Trajectory Tracking While Satisfying PTSSP

The proposed APPTC controls the AC with initial state deviations and uncertainties to finish the desired movements. The initial value for $\tilde{\boldsymbol{\alpha}}$ is set as [0.1, 0.1, 0.1]. $q = 0.01$. The control parameters are chosen as $k_1 = 0.01$ and $k_2 = 0.01$.

The states θ_1 and θ_2 under the proposed APPTC is illustrated in Fig. 5, which also shows the desired trajectories P_1 and P_2 obtained by (2). Even though certain state deviations are observed at the beginning, the states are guided to the desired trajectories, and they are tracked well. The linear quadratic Gaussian (LQG) used is designed based on the linearized model of the AC with the start states, and the control gain matrix $\boldsymbol{K}$ and the Kalman filter gain matrix $\boldsymbol{L}$ are set as

$$\boldsymbol{K} = \begin{bmatrix} 481.61 & -481.51 & 602.94 & -590.87 \\ -7336.53 & 7337.94 & -8652.23 & 8827.36 \end{bmatrix}.$$

and

$$\boldsymbol{L} = \begin{bmatrix} 31.62 & 0.0018 & 0.33 & -0.51 \\ 0.0018 & 31.64 & 0.17 & 1.01 \\ 0.33 & 0.17 & 31.62 & 0.0054 \\ -0.51 & 1.01 & 0.0054 & 31.65 \end{bmatrix}.$$

The results by LQG are also drawn in Fig. 5 as comparison. LQG cannot drive the states to follow the desired trajectories due to the strong nonlinearities of the AC.

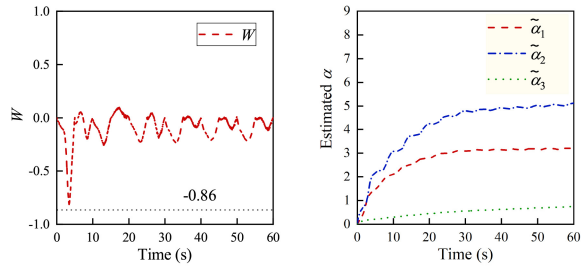

Fig. 6. (a) W and (b) $\tilde{\boldsymbol{\alpha}}$ with initial state deviations and uncertainties.

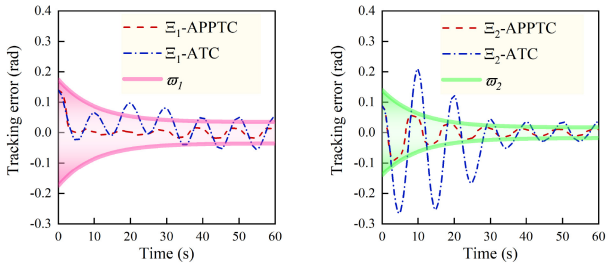

Fig. 7. Tracking errors with initial state deviations and uncertainties. (a) θ_1. (b) θ_2.

Fig. 6(a) shows the time history of W. It can be seen that $W \geq -0.86$. Therefore, σ can be -0.86, and Assumption 2 is verified. Fig. 6(b) shows the history of $\tilde{\boldsymbol{\alpha}}$. It can be seen that $\tilde{\boldsymbol{\alpha}}$ increases at the beginning and is then kept near certain values. $\tilde{\boldsymbol{\alpha}}$ is to estimate $\boldsymbol{\alpha}$, which is related to the boundaries of uncertainties. When the tracking error is large, the first term in the RHS of (18) is dominant; thus, $\tilde{\boldsymbol{\alpha}}$ increases, reducing the tracking error. When the tracking error becomes small, the second one becomes dominant and prevents the further changing of $\tilde{\boldsymbol{\alpha}}$.

The performance index of the AC system is represented by the tracking errors Ξ_1 and Ξ_2, as illustrated in Fig. 7. The PTSSP ϖ_1 and ϖ_2 are the limitations for the tracking errors. Furthermore, the adaptive tracking control for the AC system (1) is named as ATC, which is a simplified APPTC without state transformation. The tracking errors of the ATC are also shown in Fig. 7 as a comparison. It can be seen that the APPTC can guarantee the AC system satisfying PTSSP; however, the ATC generates slight larger tracking errors, exceeding the restricted area from time to time. Fig. 8 shows the control effort by two control methods. The two controls exhibit a similar control effort; however, from Fig. 8(b) the forces of APPTC have a smaller vibration amplitude than that of ATC.

In summary, the proposed APPTC can drive the motion of AC to satisfy PTSSP in the presence of initial state deviations and uncertainties.

B. Balance of System Performance and Control Effort

As discussed by the theoretical development in Section V, k_1 and k_2 are two players in the Nash game and the Nash game optimization is further demonstrated in this section. $D[\sigma] = -0.86$, $D[\boldsymbol{\varepsilon}(t_s)] = 3.6147$, $D[\|\boldsymbol{\alpha}\|] = 6.0947$, and $D[\|\tilde{\boldsymbol{\alpha}}(t_s) - \boldsymbol{\alpha}\|] = 5.9462$.

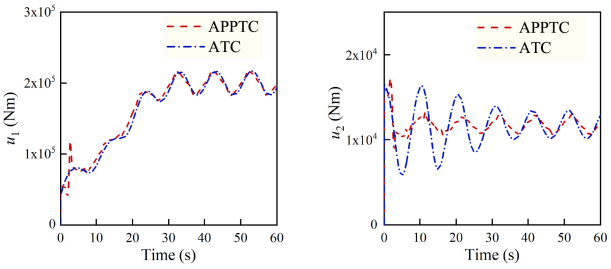

Fig. 8. Control effort (a) u_1 and (b) u_2 with initial state deviations and uncertainties.

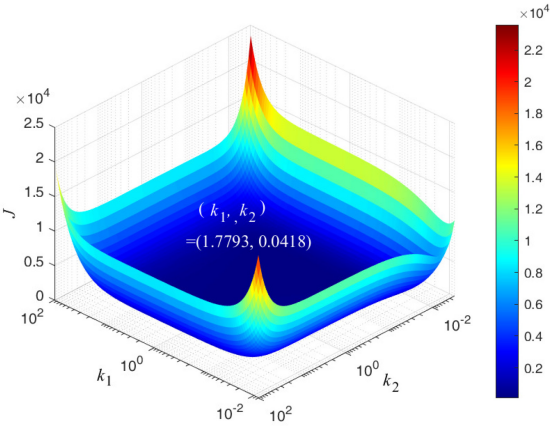

Fig. 9. Graph of J against k_1 and k_2.

Fig. 9 shows the graph of J against k_1 and k_2. By Theorem 2, the solution of the minimum value of J is the solution of the Nash equilibrium, thus $(k_1^*, k_2^*) = (1.7793, 0.0418)$. Fig. 9 echoes the fact that the Nash equilibrium of the game formulated in Section V always exists.

Fig. 10 describes how a player's choice affects his/her cost if the other player is assumed at the Nash equilibrium. Fig. 10(a) illustrates the cost J_1 against different k_1 when the player k_2 is at the Nash equilibrium k_2^*. In this situation, it can be seen that the best choice of player k_1 is $k_1^* = 1.7793$. Fig. 10(b) illustrates the cost J_2 against different k_2 in the event that the player k_1 stays at the k_1^*. In this situation, the best choice of player k_2 is $k_2^* = 0.0418$. A salient feature of the Nash equilibrium is that no player can benefit by changing decision from the Nash equilibrium while the other players keep theirs unchanged.

To compare the Nash game optimization to the commonly used optimization with a single objective, the costs J_1 and J_2 corresponding to different optimizing solutions are drawn in Fig. 11. The superscripts "o1" and "o2" denote the solutions for global minimum J_1 and J_2, respectively. To obtain global minimum J_1, $(k_1^{o1}, k_2^{o1}) = (1.1550, 0.4522)$, while the solution for a global minimum J_1 is $(k_1^{o2}, k_2^{o2}) = (402.0830, 0.4550)$. The Nash equilibrium is not the same as the global minimum points of J_1 and J_2, as the two players are noncooperative. To reach the global minimum J_2, the

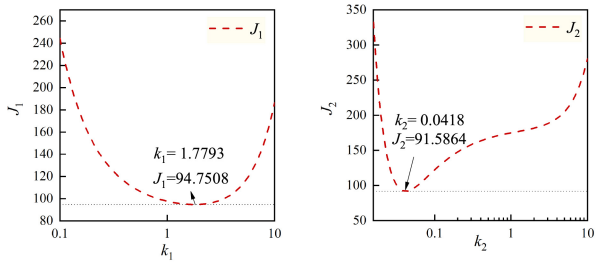

Fig. 10. Costs (a) J_1 and (b) J_2 corresponding to different player choices.

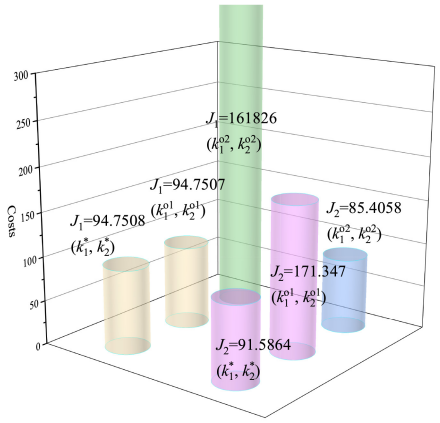

Fig. 11. Costs J_1 and J_2 corresponding to different optimizing solutions.

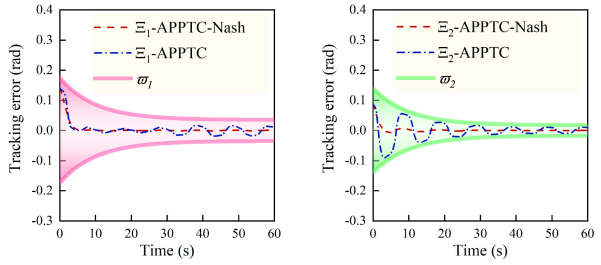

Fig. 12. Tracking errors for (a) θ_1 and (b) θ_2 with the Nash game optimization.

player has to pay $k_1^{o2} = 402.0830$, which is unlikely happen in practice.

Fig. 12 plots the tracking errors of the APPTC with the Nash equilibrium, compared to the arbitrarily chosen decision couple in Section VI-A. It can be seen that the tracking errors of the APPTC with the Nash equilibrium are much smaller. These results demonstrate the benefit of balancing the system performance and control effort by fuzzy optimality.

VII. Conclusion

The main challenges of precise tracking control for an AC are the strong nonlinearities and uncertainties of the dynamic system. For this, an APPTC design is carried out to render AC to fulfill the task of precise tracking control by satisfying PTSSP. Lyapunov analysis proves the uniform boundedness and uniform ultimate boundedness of the APPTC and indicates the tunable parameters on the system performance. Furthermore, we form a fuzzy optimality by a Nash game of two control parameters, prove the existence of the Nash equilibrium by theoretical analysis, and provide the procedure to obtain the Nash equilibrium. The comparison demonstrates the effectiveness of the proposed APPTC on precise tracking control. The results of fuzzy optimality by the Nash game illustrate the benefit of balancing the system performance and control effort. Future explorations for optimal design in controlling AC using type-2 fuzzy set are worth pursuing, being more comprehensive in representing uncertainties compared with the type-1 fuzzy set herein.

Appendix A
AC Model Matrixes Elements

The elements of AC model are

$$M_{11} = m\Big((l_2 - l_1)^2 + 2l_1(l_1 - l_2C_2)\Big) + l_1^2 m_1/3 + m_2\Big(2l_2^2 + 6l_1(l_1 - l_2C_2)\Big)/6$$
$$M_{12} = M_{21} = l_2(2l_2(3m + m_2) - 3l_1C_2(2m + m_2))/6$$
$$M_{22} = l_2^2(3m + m_2)/3$$

where $C_2 = \cos\theta_2$, $C_1 = \cos\theta_1$, $S_2 = \sin\theta_2$, $S_1 = \sin\theta_1$

$$\begin{aligned} &M_{11}M_{22} - M_{12}M_{21} \\ &= 2l_2^2m^2l_1(l_1 - l_2C_2) + \frac{2m_2l_2^2ml_1(l_1 - l_2C_2)}{3} \\ &\quad - l_1^2l_2^2m^2C_2^2 - l_1^2m_2l_2^2mC_2^2 - \frac{l_1^2m_2^2l_2^2C_2^2}{4} \\ &\quad + 2l_1l_2^3m^2C_2 + \frac{2l_1m_2l_2^3mC_2}{3} - 2l_1l_2^3m^2 \\ &\quad + l_1^2l_2^2m^2 - \frac{2l_1m_2l_2^3m}{3} + \frac{4l_1^2m_2l_2^2m}{3} + \frac{l_1^2m_2^2l_2^2}{3} \\ &= \frac{4l_1^2m_2l_2^2m + l_1^2m_2^2l_2^2}{12} \\ &\quad + \frac{\big(12l_1^2l_2^2m^2 + 12l_1^2m_2l_2^2m + 3l_1^2m_2^2l_2^2\big)S_2^2}{12} \\ &\quad + \frac{\big(24l_2^2m^2 + 8m_2l_2^2m\big)l_1(l_1 - l_2)}{12} > 0. \end{aligned}$$

$$C_{11} = l_2l_1(2m + m_2)S_2\theta_2', \quad C_{22} = 0$$
$$C_{12} = C_{21} = -\frac{1}{2}l_2l_1(2m + m_2)S_2\theta'$$
$$G_1 = gl_1mC_\theta + \frac{1}{2}gl_1C_\theta m_1 + gl_1C_\theta m_2 + \frac{1}{2}gl_2(2m + m_2)\big(S_\theta S_{\theta_2} - C_\theta C_2\big)$$
$$G_2 = \frac{1}{2}l_2g(2m + m_2)(S_\theta S_2 - C_\theta C_2).$$

Appendix B
Transformed System Elements

The elements of transformed system are $\Upsilon\dot{x} + \Gamma = [y_1, y_2]^T$, and

$$y_1 = -\frac{2(H_{11})x_1\varpi_1\dot{x}_1^2}{3\pi\left(x_1^2 + 1\right)^2} + \frac{\dot{x}_1}{6}H_{12} + \frac{1}{6}(H_{13})\dot{x}_2^2 + \frac{1}{6}(H_{14}) + \frac{1}{6}(H_{15})\dot{x}_2$$

$$y_2 = \frac{1}{6}l_2(H_{21}) + \frac{4l^2(3m+m_2)\dot{\varpi}_2\dot{x}_2}{3\left(\pi x_2^2+\pi\right)} + \frac{1}{6}l_2\dot{x}_1(H_{22}) - \frac{4l^2(3m+m_2)\varpi_2 x_2\dot{x}_2^2}{3\pi\left(x_2^2+1\right)^2} + \frac{1}{6}l_2\dot{x}_1^2(H_{23})$$

where

$$\begin{aligned}
H_{11} &= 2m_1l_1^2 - 6l_2C_{P2}(2m+m_2)l_1 + 6\left(l_2^2+l_1^2\right)m + 2\left(l_2^2+3l_1^2\right)m_2\\
H_{12} &= \frac{12l_2l_1S_{P2}(2m+m_2)\varpi_1\dot{P}_2}{\pi x_1^2+\pi} + \frac{4(H_{16})\dot{\varpi}_1}{\pi x_1^2+\pi} + \frac{24l_2l_1\arctan(x_2)S_{P2}(2m+m_2)\varpi_1\dot{\varpi}_2}{\pi\left(\pi x_1^2+\pi\right)} + \frac{4l_2l_1S_{P2}(2m+m_2)\varpi_1\varpi_2\dot{x}_2}{\left(\pi x_1^2+\pi\right)\left(\pi x_2^2+\pi\right)}\\
H_{13} &= \frac{12l_2l_1S_{P2}(2m+m_2)\varpi_2^2}{\left(\pi x_2^2+\pi\right)^2} - \frac{4l_2(6l_2m+2l_2m_2-3l_1C_{P2}(2m+m_2))x_2\varpi_2}{\pi\left(x_2^2+1\right)^2}\\
H_{14} &= 3l_2l_1S_{P2}(2m+m_2)\dot{P}_2^2 + 6l_2l_1S_{P2}(2m+m_2)\dot{P}_1\dot{P}_2 + \frac{12l_2l_1\arctan(x_1)S_{P2}(2m+m_2)\dot{P}_2}{\pi}(\dot{\varpi}_1+\dot{\varpi}_2)\\
&\quad + \frac{12l_2l_1\arctan(x_2)^2S_{P2}(2m+m_2)\dot{\varpi}_2^2}{\pi^2} + 6gl_1mC_{P1} + 3gl_1C_{P1}m_1 + 6gl_1C_{P1}m_2\\
&\quad - 3gl_2C_{P1}C_{P2}(2m+m_2) + 3gl_2S_{P1}S_{P2}(2m+m_2) + \frac{12l_2l_1\arctan(x_2)S_{P2}(2m+m_2)\dot{P}_1\dot{\varpi}_2}{\pi}\\
&\quad + \frac{24l_2l_1\arctan(x_1)\arctan(x_2)S_{P2}(2m+m_2)\dot{\varpi}_1\dot{\varpi}_2}{\pi^2} + (H_{17})\ddot{P}_1 + l_2(6l_2m+2l_2m_2-3l_1C_{P2}(2m+m_2))\ddot{P}_2\\
&\quad + \frac{2\arctan(x_1)(H_{18})\ddot{\varpi}_1}{\pi} + \frac{2l_2\arctan(x_2)(6l_2m+2l_2m_2-3l_1C_{P2}(2m+m_2))\ddot{\varpi}_2}{\pi}\\
H_{15} &= \frac{12l_2l_1S_{P2}(2m+m_2)\varpi_2}{\pi x_2^2+\pi}\left(\dot{P}_1+\dot{P}_2\right) + \frac{24l_2l_1\arctan(x_1)S_{P2}(2m+m_2)\varpi_2}{\pi\left(\pi x_2^2+\pi\right)}(\dot{\varpi}_1+\dot{\varpi}_2) + \frac{4l_2(6l_2m+2l_2m_2-3l_1C_{P2}(2m+m_2))\dot{\varpi}_2}{\pi x_2^2+\pi}\\
H_{16} &= 2m_1l_1^2 - 6l_2C_{P2}(2m+m_2)l_1 + 6\left(l_2^2+l_1^2\right)m + 2\left(l_2^2+3l_1^2\right)m_2\\
H_{17} &= 2m_1l_1^2 - 6l_2C_{P2}(2m+m_2)l_1 + 6\left(l_2^2+l_1^2\right)m + 2\left(l_2^2+3l_1^2\right)m_2\\
H_{18} &= 2m_1l_1^2 - 6l_2C_{P2}(2m+m_2)l_1 + 6\left(l_2^2+l_1^2\right)m + 2\left(l_2^2+3l_1^2\right)m_2.\\
H_{21} &= 3g(2m+m_2)S_{P1}S_{P2} - 3g(2m+m_2)C_{P1}C_{P2} + \ddot{P}_1(2l_2(3m+m_2)-3l_1(2m+m_2)C_{P2}) + \frac{2\ddot{\varpi}_1\arctan(x_1)(2l_2(3m+m_2)-3l_1(2m+m_2)C_{P2})}{\pi}\\
&\quad + 2l_2(3m+m_2)\ddot{P}_2 + \frac{4l_2(3m+m_2)\ddot{\varpi}_2\arctan(x_2)}{\pi} - \frac{12l_1(2m+m_2)\dot{P}_1\dot{\varpi}_1\arctan(x_1)S_{P2}}{\pi} - 3l_1(2m+m_2)\dot{P}_1^2S_{P2}\\
&\quad - \frac{12l_1(2m+m_2)\dot{\varpi}_1^2\arctan(x_1)^2S_{P2}}{\pi^2}\\
H_{22} &= \frac{4\dot{\varpi}_1(2l_2(3m+m_2)-3l_1(2m+m_2)C_{P2})}{\pi x_1^2+\pi} - \frac{12l_1(2m+m_2)\varpi_1\dot{P}_1S_{P2}}{\pi x_1^2+\pi} - \frac{24l_1(2m+m_2)\varpi_1\dot{\varpi}_1\arctan(x_1)S_{P2}}{\pi\left(\pi x_1^2+\pi\right)}\\
H_{23} &= -\frac{4\varpi_1x_1(2l_2(3m+m_2)-3l_1(2m+m_2)C_{P2})}{\pi\left(x_1^2+1\right)^2} - \frac{12l_1(2m+m_2)\varpi_1^2S_{P2}}{\left(\pi x_1^2+\pi\right)^2}.\\
C_{P1} &= \cos\left(P_1+\frac{2\arctan(x_1)\varpi_1}{\pi}\right)\\
S_{P1} &= \sin\left(P_1+\frac{2\arctan(x_1)\varpi_1}{\pi}\right)\\
C_{P2} &= \cos\left(P_2+\frac{2\arctan(x_2)\varpi_2}{\pi}\right)\\
S_{P2} &= \sin\left(P_2+\frac{2\arctan(x_2)\varpi_2}{\pi}\right).
\end{aligned}$$

APPENDIX C
D-OPERATION

Consider a fuzzy set $S = (\delta, \mu(\delta)) \mid \delta \in \Omega_\delta$. For any function $f : \Omega_\delta \to R$, the D-operation $D[f(\delta)]$ can be expressed as

$$D\left[f(\delta)\right] = \frac{\int_{\Omega_\delta} f(\delta)\mu(\delta)d\delta}{\int_{\Omega_\delta}\mu(\delta)d\delta}.$$

For any crisp constant $h \in R$

$$D\left[hf(\delta)\right] = hD\left[f(\delta)\right].$$

APPENDIX D
COST FUNCTIONS ELEMENTS

The elements of cost functions are

$$\begin{aligned}
\epsilon_1 &= D[\|\boldsymbol{\varepsilon}(t_s)\|]^4\\
\epsilon_2 &= 4(1+D[\sigma])^2\\
\epsilon_3 &= -4(1+D[\sigma])D[\|\boldsymbol{\varepsilon}(t_s)\|]^2\\
\epsilon_4 &= \frac{(1+D[\sigma])^2\left(qD[\|\boldsymbol{\alpha}\|]^2+2-4D\left[\left\|\tilde{\boldsymbol{\alpha}}(t_s)-\boldsymbol{\alpha}\right\|^2\right]\right)}{4}\\
\epsilon_5 &= -D[\|\boldsymbol{\varepsilon}(t_s)\|]^2 (1+D[\sigma])\left(2qD[\|\boldsymbol{\alpha}\|]^2+\left(1-2D\left[\left\|\tilde{\boldsymbol{\alpha}}(t_s)-\boldsymbol{\alpha}\right\|^2\right]\right)\right)\\
\epsilon_6 &= q^2\left((1+D[\sigma])\left(D[\|\boldsymbol{\alpha}\|]^2+50\left(1-2D\left[\left\|\tilde{\boldsymbol{\alpha}}(t_s)-\boldsymbol{\alpha}\right\|^2\right]\right)\right)\right)^2\\
\epsilon_7 &= 4(1+D[\sigma])^2\\
\epsilon_8 &= (1+D[\sigma])^2\left(4qD[\|\boldsymbol{\alpha}\|]^2+2\right)\\
\epsilon_9 &= q^2(1+D[\sigma])^2\left(D[\|\boldsymbol{\alpha}\|]^2+50\right)^2.
\end{aligned}$$

REFERENCES

[1] M. Deng, A. Ji, L. Zhang, H. Wang, and Z. Zhao, "Lateral vibration behaviors of the straight boom of the aerial work platform in the horizontal linear motion," *Autom. Constr.*, vol. 134, Feb. 2022, Art. no. 104095. [Online]. Available: https://doi.org/10.1016/j.autcon.2021.104095

[2] H. Ouyang, Z. Tian, L. Yu, and G. Zhang, "Motion planning approach for payload swing reduction in tower cranes with double-pendulum effect," *J. Franklin Inst.*, vol. 357, pp. 8299–8320, Sep. 2020.

[3] Y. Liu, Y. Mei, H. Cai, C. He, T. Liu, and G. Hu, "Asymmetric input–output constraint control of a flexible variable-length rotary crane arm," *IEEE Trans. Cybern.*, vol. 52, no. 10, pp. 10582–10591, Oct. 2022, doi: 10.1109/TCYB.2021.3055151.

[4] Y. Wen, X. Lou, W. Wu, and B. Cui, "Backstepping boundary control for a class of gantry crane systems," *IEEE Trans. Cybern.*, early access, Aug. 9, 2022, doi: 10.1109/TCYB.2022.3188494.

[5] Y. Mei, Y. Liu, H. Wan, and H. Cai, "Adaptive deformation control of a flexible variable-length rotary crane arm with asymmetric input–output constraints," *IEEE Trans. Cybern.*, vol. 52, no. 12, pp. 13752–13761, Dec. 2022, doi: 10.1109/TCYB.2021.3112706.

[6] C. P. Bechlioulis and G. A. Rovithakis, "Robust adaptive control of feedback linearizable MIMO nonlinear systems with prescribed performance," *IEEE Trans. Autom. Control*, vol. 53, no. 9, pp. 2090–2099, Oct. 2008.

[7] C. Wei, Q. Chen, J. Liu, Z. Yin, and J. Luo, "An overview of prescribed performance control and its application to spacecraft attitude system," *Proc. Inst. Mech. Eng. I, J. Syst. Control Eng.*, vol. 235, no. 4, pp. 435–447, 2021.

[8] L. Sun, H. Cao, and Y. Song, "Prescribed performance control of constrained Euler–Language systems chasing unknown targets," *IEEE Trans. Cybern.*, early access, Jan. 26, 2022, doi: 10.1109/TCYB.2021.3134819.

[9] H. Ma, Q. Zhou, H. Li, and R. Lu, "Adaptive prescribed performance control of a flexible-joint robotic manipulator with dynamic uncertainties," *IEEE Trans. Cybern.*, vol. 52, no. 12, pp. 12905–12915, Dec. 2022.

[10] L. Zhang, W.-W. Che, B. Chen, and C. Lin, "Adaptive fuzzy output-feedback consensus tracking control of nonlinear multiagent systems in prescribed performance," *IEEE Trans. Cybern.*, vol. 53, no. 3, pp. 1932–1943, Mar. 2023.

[11] H. Yin, Y.-H. Chen, D. Yu, H. Lü, and W. Shangguan, "Adaptive robust control for a soft robotic snake: A smooth-zone approach," *Appl. Math. Model.*, vol. 80, pp. 454–471, Apr. 2020. [Online]. Available: https://doi.org/10.1016/j.apm.2019.11.015

[12] Y.-H. Chen and X. Zhang, "Adaptive robust approximate constraint-following control for mechanical systems," *J. Franklin Inst.*, vol. 347, no. 1, pp. 69–86, 2010.

[13] Q. Sun, X. Wang, G. Yang, Y.-H. Chen, and F. Ma, "Adaptive robust formation control of connected and autonomous vehicle swarm system based on constraint following," *IEEE Trans. Cybern.*, early access, Feb. 23, 2022, doi: 10.1109/TCYB.2022.3150032.

[14] Z. Zhang, J. Zhang, H. Yin, B. Zhang, and X. Jing, "Bio-inspired structure reference model oriented robust full vehicle active suspension system control via constraint-following," *Mech. Syst. Signal Process.*, vol. 179, Nov. 2022, Art. no. 109368.

[15] Q. Sun, G. Yang, X. Wang, and Y.-H. Chen, "Regulating constraint-following bound for fuzzy mechanical systems: Indirect robust control and fuzzy optimal design," *IEEE Trans. Cybern.*, vol. 52, no. 7, pp. 5868–5881, Jul. 2022, doi: 10.1109/TCYB.2020.3040680.

[16] Z. Zhang, A. Qin, J. Zhang, B. Zhang, Q. Fan, and N. Zhang, "Fuzzy sampled-data H∞ sliding-mode control for active hysteretic suspension of commercial vehicles with unknown actuator-disturbance," *Control Eng. Pract.*, vol. 117, Dec. 2021, Art. no. 104940.

[17] C. P. Bechlioulis and G. A. Rovithakis, "Robust partial-state feedback prescribed performance control of cascade systems with unknown nonlinearities," *IEEE Trans. Autom. Control*, vol. 56, no. 9, pp. 2224–2230, Sep. 2011.

[18] S. Gao, H. Dong, B. Ning, and Q. Zhang, "Cooperative prescribed performance tracking control for multiple high-speed trains in moving block signaling system," *IEEE Trans. Intell. Transp. Syst.*, vol. 20, no. 7, pp. 2740–2749, Jul. 2019.

[19] Y.-H. Chen, "Constraint-following servo control design for mechanical systems," *J. Vib. Control*, vol. 15, no. 3, pp. 369–389, 2009.

[20] F. E. Udwadia and R. E. Kalaba, "A new perspective on constrained motion," *Proc. Roy. Soc. A, Math. Phys. Eng. Sci.*, vol. 439, no. 1906, pp. 407–410, Nov. 1992 doi: 10.1098/RSPA.1992.0158.

[21] F. E. Udwadia and R. E. Kalaba, *Analytical Dynamics: A New Approach*. Cambridge, U.K.: Cambridge Univ. Press, 1996.

[22] M. Zheng, B. Zhang, J. Zhang, and N. Zhang, "Physical parameter identification method based on modal analysis for two-axis on-road vehicles: Theory and simulation," *Chin. J. Mech. Eng.*, vol. 29, no. 4, pp. 756–764, Jul. 2016, doi: 10.3901/CJME.2016.0108.004.

[23] Z. Zhang, J. Zhang, J. Dai, B. Zhang, and H. Qi, "A fusion algorithm for estimating time-independent/-dependent parameters and states," *Sensors*, vol. 21, no. 12, p. 4068, 2021.

[24] S. Pincus and R. E. Kalman, "Not all (possibly) 'random' sequences are created equal," *Proc. Nat. Acad. Sci.*, vol. 94, no. 8, pp. 3513–3518, 1997.

[25] Y.-H. Chen, "Optimal design of robust control for uncertain systems: A fuzzy approach," *Nonlinear Dyn. Syst. Theory*, vol. 1, no. 2, pp. 133–143, 2001.

[26] Y.-H. Chen, "A new approach to the control design of fuzzy dynamical systems," *J. Dyn. Syst. Meas. Control*, vol. 133, no. 6, 2011, Art. no. 61019, doi: 10.1115/1.4004579.

[27] H. Yin, Y.-H. Chen, and D. Yu, "Vehicle motion control under equality and inequality constraints: A diffeomorphism approach," *Nonlinear Dyn.*, vol. 95, no. 1, pp. 175–194, 2019.

[28] H. Yin, Y.-H. Chen, D. Yu, and H. Lü, "Nash-game-oriented optimal design in controlling fuzzy dynamical systems," *IEEE Trans. Fuzzy Syst.*, vol. 27, no. 8, pp. 1659–1673, Aug. 2019.

[29] Y. Cui, H. Feng, W. Zhang, Z. Shu, and T. Huang, "Positivity and stability analysis of T–S fuzzy descriptor systems with bounded and unbounded time-varying delays," *IEEE Trans. Cybern.*, vol. 52, no. 11, pp. 11649–11660, Nov. 2022, doi: 10.1109/TCYB.2021.3072392.

[30] M. Zhang and X. Jing, "A bioinspired dynamics-based adaptive fuzzy SMC method for half-car active suspension systems with input dead zones and saturations," *IEEE Trans. Cybern.*, vol. 51, no. 4, pp. 1743–1755, Apr. 2021, doi: 10.1109/TCYB.2020.2972322.

[31] Q. Liao and D. Sun, "Sparse and decoupling control strategies based on Takagi–Sugeno fuzzy models," *IEEE Trans. Cybern.*, vol. 51, no. 2, pp. 947–960, Feb. 2021, doi: 10.1109/TCYB.2019.2896530.

[32] R. Zhang, D. Zeng, J. H. Park, H.-K. Lam, and X. Xie, "Fuzzy sampled-data control for synchronization of T–S fuzzy reaction–diffusion neural networks with additive time-varying delays," *IEEE Trans. Cybern.*, vol. 51, no. 5, pp. 2384–2397, May 2021, doi: 10.1109/TCYB.2020.2996619.

[33] B.-S. Chen, M.-Y. Lee, T.-H. Lin, and W. Zhang, "Robust state/fault estimation and fault-tolerant control in discrete-time T–S fuzzy systems: An embedded smoothing signal model approach," *IEEE Trans. Cybern.*, vol. 52, no. 7, pp. 6886–6900, Jul. 2022, doi: 10.1109/TCYB.2020.3042984.

[34] H. Yin, Y.-H. Chen, and D. Yu, "Stackelberg-theoretic approach for performance improvement in fuzzy systems," *IEEE Trans. Cybern.*, vol. 50, no. 5, pp. 2223–2236, May 2020.

[35] W. Wang, H. Liang, Y. Pan, and T. Li, "Prescribed performance adaptive fuzzy containment control for nonlinear multiagent systems using disturbance observer," *IEEE Trans. Cybern.*, vol. 50, no. 9, pp. 3879–3891, Sep. 2020.

[36] X. Chen, H. Zhao, S. Zhen, and H. Sun, "Novel optimal adaptive robust control for fuzzy underactuated mechanical systems: A Nash game approach," *IEEE Trans. Fuzzy Syst.*, vol. 29, no. 9, pp. 2798–2809, Sep. 2021, doi: 10.1109/TFUZZ.2020.3007452.

[37] C. Li, H. Zhao, S. Zhen, and Y.-H. Chen, "Control design with optimization for fuzzy steering-by-wire system based on Nash game theory," *IEEE Trans. Cybern.*, vol. 52, no. 8, pp. 7694–7703, Aug. 2022, doi: 10.1109/TCYB.2021.3050509.

Zheshuo Zhang (Member, IEEE) received the Ph.D. degree from the School of Civil Engineering and Built Environment, Queensland University of Technology, Brisbane, QLD, Australia, in 2019, and the M.E. degree from the College of Mechanical and Vehicle Engineering, Hunan University, Changsha, China, in 2015.

He is an Associate Researcher with Zhejiang University City College, Hangzhou, China. He was a Research Fellow with the College of Mechanical and Vehicle Engineering, Hunan University. His research interests include trajectory planning, structure optimization, adaptive robust control, and precise control of uncertain nonlinear systems.

Bangji Zhang received the B.E. degree in mechanical engineering from Jilin University, Changchun, China, in 1992, and the M.E. and Ph.D. degrees in mechanical engineering from Hunan University, Changsha, China, in 1999 and 2010, respectively.

He was a Visiting Scholar with the University of Technology Sydney, Ultimo, NSW, Australia, from 2013 to 2014. He is a Professor with Zhejiang University City College, Hangzhou, China. He previously served as a Professor with the College of Mechanical and Vehicle Engineering, Hunan University, and as a Visiting Scholar with the University of Technology Sydney. His research interests include intelligent vehicle and nonlinear systems vibration control.

Dongpu Cao (Member, IEEE) received the Ph.D. degree from Concordia University, Montréal, QC, Canada, in 2008.

He is a Professor with Tsinghua University, Beijing, China. His current research focuses on driver cognition, automated driving, and cognitive autonomous driving. He has contributed more than 200 papers and three books.

Prof. Cao received the SAE Arch T. Colwell Merit Award in 2012, the IEEE VTS 2020 Best Vehicular Electronics Paper Award, and six Best Paper Awards from international conferences. He has served as a Deputy Editor-in-Chief for *IET Intelligent Transport Systems*, and an Associate Editor for IEEE TRANSACTIONS ON VEHICULAR TECHNOLOGY, IEEE TRANSACTIONS ON INTELLIGENT TRANSPORTATION SYSTEMS, IEEE/ASME TRANSACTIONS ON MECHATRONICS, IEEE TRANSACTIONS ON INDUSTRIAL ELECTRONICS, IEEE/CAA JOURNAL OF AUTOMATICA SINICA, IEEE TRANSACTIONS ON COMPUTATIONAL SOCIAL SYSTEMS, and *Journal of Dynamic Systems, Measurement and Control (ASME)*. He is an IEEE VTS Distinguished Lecturer.

Hui Yin (Member, IEEE) received the B.S. and Ph.D. degrees in mechanical engineering from Hunan University, Changsha, China, in 2012 and 2018, respectively.

From 2016 to 2018, he was a Visiting Scholar with the George W. Woodruff School of Mechanical Engineering, Georgia Institute of Technology, Atlanta, GA, USA. He is currently an Associate Professor with the College of Mechanical and Vehicle Engineering, Hunan University. His research interests include mechanical system dynamics, robust control, adaptive robust control, fuzzy engineering, and uncertainty management.